

University of Denver

**Digital Commons @ DU**

---

Fuel Efficiency Automobile Test Publications

Fuel Efficiency Automobile Test Data Repository

---

2004

## **Infrared Thermal Imaging of Automobiles: Identification of Cold Start Vehicles**

Angela M. Monateri

Donald H. Stedman

Follow this and additional works at: [https://digitalcommons.du.edu/feat\\_publications](https://digitalcommons.du.edu/feat_publications)



Part of the **Environmental Chemistry Commons**

---

# **Infrared Thermal Imaging of Automobiles: Identification of Cold Start Vehicles**

**Angela M. Monateri and Donald H. Stedman**

**Department of Chemistry and Biochemistry  
University of Denver  
Denver, CO 80208**

**August 2004**

**Prepared for:**

**Attn: Niranjan Vescio  
ESP  
2002 North Forbes Blvd.  
Tucson, AZ 85745-1446**

## **Abstract**

An automobile's emissions can be determined remotely by means of on-road remote sensing. Remote sensors correctly identify vehicles in a cold-start mode, which have no repairable fault, as relatively high emitters of pollution. For this reason it is desirable in a "high emitter identification" program to remove cold cars from the data base. Infrared thermal imaging of automobiles has the potential to determine if a car is hot or cold (i.e. a car that has just been started would be cold compared to a car that has been operating for several minutes.) With a low-cost infrared camera, thermal images of numerous vehicles and their surroundings were taken to evaluate this potential. Amongst other observables, the reflection of heat from the underbody of the car reflecting off the road surface can be seen. A hot vehicle has a strong reflection, while a cold car has almost no reflection from the underbody. Thus, the difference between a cold vehicle, versus a fully warmed up vehicle can be determined. The parameters optimized in this study include: how to set up the camera to optimize observable reflection, the signatures of hot and cold cars and how to tell the difference, how the weather, the sun, and the driving surface can affect the thermal images. A reanalysis of data from dynamometer studies resulted in an average warm-up time for newer vehicles of 25 +/- 12.5 seconds.

# Table of Contents

Introduction.....	1
Exhaust Chemistry.....	1
Hot and Cold Vehicle Studies.....	5
Fuel Efficiency Automobile Test (FEAT).....	14
History of Infrared Radiation.....	17
Blackbody Radiation.....	19
Experimental Set-up of Infrared Camera.....	22
Infrared Camera.....	22
Thermal Image Set-up.....	22
On-road Set-up.....	25
Road Surface Temperature.....	26
Initial Experiments.....	26
Cold Road Conditions.....	27
Hot Road Conditions.....	28
Hot Road Cold Start.....	29
FEAT Set-up.....	31
Cold Start with FEAT.....	32
Regis High School Study.....	32
Analysis of the Infrared Images.....	35
Reanalysis of CE-CERT FTP Data.....	36
Results and Discussion.....	38
Initial Set-up Images.....	38
Cold Start Images.....	44
Images on Cold Road Surfaces.....	48
Effects of Snow on Road Surfaces.....	53
Images on Hot Road Surfaces.....	56
Cold Start Images on Hot Road Surfaces.....	61
Results from the Regis High School Experiments.....	65
Comparison of Cold Starts.....	72
Quantitative Analysis of the Infrared Images.....	72
Reanalysis of Data from Younglove, <i>et al.</i> .....	75

Conclusion.....	81
Future Research and Development.....	83
References.....	84

# List of Figures

**Figure 1.** FTP Driving Cycle speed- time trace.<sup>11</sup> This trace of the FTP cycle does not include the ten minute soak time between the transient phase and the hot start phase.....7

**Figure 2.** US06 Driving Cycle speed-time trace.<sup>11</sup> .....8

**Figure 3.** Mean catalyst light off time by model year for a) CO, b) HC, and c) NOx from Younglove *et al.*<sup>13</sup> .....11

**Figure 4.** Typical layout of a remote sensing instrument observing vehicles across a single lane of traffic.<sup>12</sup> .....14

**Figure 5.** Blackbody radiation curves. The x-axis is the wavelength in  $\mu\text{m}$ , and the y-axis is the spectral radiant emittance ( $\text{W}/\text{cm}^2 \times 10^3$ ).<sup>7</sup> .....19

**Figure 6.** Planck Distribution. The x-axis is the wavelength in  $\mu\text{m}$ , and the y-axis is the spectral radiant emittance ( $\text{W}/\text{cm}^2 \times 10^3$ ).<sup>7</sup> .....21

**Figure 7.** Schematic diagram of the top of the FLIR camera. 1) SEL Button, used to adjust the camera scale in manual mode. 2) FRZ Button, used to start the camera mode and can be used to freeze an image on the screen and can save images to the camera when pressed for longer than a second. 3) Navigation Pad, used to navigate the menu options. 4) YES Button, used to display the menu, select a menu option. 5) NO Button, used to unfreeze an image, leave menu options.<sup>7</sup> .....24

**Figure 8.** Camera set-up on Flamingo Road in Las Vegas, Nevada.....29

**Figure 9.** Set-up in DRI parking lot for observing the cold start vehicle warming up as it was driven around the parking lot.....30

**Figure 10.** Schematic drawing of FEAT unit and the infrared camera set-up.<sup>6</sup> .....31

**Figure 11.** Pictures of the FEAT set-up at Regis High School. (A) Looking north at the source. (B) looking east along the access road towards the school.....34

<b>Figure 12A-E.</b> Infrared images using the Iron palate with the auto adjust on. After the first vehicle passes in front of the camera the image darkens and takes several seconds to adjust back to the same scale as the first image.....	41
(A) Initial vehicle driving past the camera.....	39
(B) Vehicle following the initial vehicle in quick succession, with its image much darker due to the auto adjust mode on the camera.....	39
(C) Darker image due to the camera's auto adjust mode.....	40
(D) Camera still adjusting the image.....	40
(E) The camera is no longer adjusting the scale of the image.....	41
<b>Figure 13.</b> Hot vehicle driving east on Iliff Avenue. There is a bright reflection from the underbody of the vehicle, but the tire treads cannot be seen to determine the status of the vehicle.....	43
<b>Figure 14.</b> Hot vehicle. This vehicle has both a bright reflection from the underbody of the vehicle as well as warm side walls on the tires.....	43
<b>Figure 15.</b> Cold start of Blue. The %CO is 5.66, which is a high reading for a vehicle.....	44
<b>Figure 16.</b> Blue shortly after cold start. The %CO at the time of start was 2.83. The image is darker than the following images because the camera was adjusted in between images.....	45
<b>Figure 17.</b> Blue, with %CO of 2.07. The reflection from the underbody of the vehicle is much stronger than the previous figure.....	46
<b>Figure 18.</b> Blue with 0.13 %CO. The vehicle has a much stronger reflection from the underbody of the vehicle, as well as a very bright exhaust system. The vehicle's emissions are now low enough to pass an emissions test. Blue took 223 seconds to warm up.....	46
<b>Figure 19.</b> Blue with 0.13 %CO. The vehicle would still pass an emissions test, but is still warming up.....	47
<b>Figure 20.</b> The vehicle is still emitting a constant percentage of CO in the exhaust, and is now fully warmed up.....	47

<b>Figure 21.</b> Cold vehicle. This vehicle is leaving the restricted parking lot across from the north side of Olin Hall, and has no bright underbody reflection or hot tire treads.....	49
<b>Figure 22.</b> Cold start vehicle. This SUV has a very faint reflection from the underbody of the vehicle and the tire treads do not emit very much infrared radiation.....	50
<b>Figure 23.</b> Cold start vehicle. This vehicle is leaving the metered visitor parking lot (304) across from Cherrington Hall, and the exhaust of the vehicle appears to be hot due to the small increase of heat from the vehicle starting. This vehicle has no strong reflection from the underbody of the vehicle or hot tire treads to indicate that it is warm.....	50
<b>Figure 24.</b> Warm vehicle. It is unknown if the vehicle is fully warm. If the emissions for this vehicle were known, then the status of the vehicle could then be decided.....	51
<b>Figure 25.</b> Hot truck. Has a very bright reflection under the vehicle as well as uniformly heated tire treads and sidewalls on the tires.....	51
<b>Figure 26.</b> Hot Sport Utility Vehicle. This vehicle has both hot tire treads as well as a very bright reflection from the underbody of the vehicle.....	52
<b>Figure 27.</b> Hot truck. The truck in this image has both hot tire treads and a bright reflection from the underbody of the vehicle. The reflection can be seen at a distance as long as the road surface is level.....	52
<b>Figure 28.</b> Breckenridge Ski Patrol SUV. The vehicle is hot, as can be seen by the hot engine through the grille, however because snow does not reflect IR radiation, there is no reflection on the road from the underbody of the vehicles.....	54
<b>Figure 29.</b> Warm vehicle leaving the parking lot. The exhaust system of this vehicle appears to be hot, however because there is no reflection on the road surface on the snow, the status of this vehicle cannot be clearly determined.....	54



**Figure 30.** Hot truck on snow. The exhaust system of the vehicle is hot as well as the sidewalls of the tires. In the boxed area, some of the snow has melted, and water is reflecting the sun light.....55

**Figure 31.** Cold SUV leaving the parking lot. The SUV in this figure looks very similar to the Breckinridge Ski Patrol vehicle; however the hot looking tire wall is due to heating by the sun and not by being driven. This can be determined because the other tire walls do not look hot.....55

**Figure 32.** Flamingo Road in Las Vegas, Nevada facing towards the east. The road temperature is over 120°F.....56

**Figure 33.** Traffic on Flamingo Road. The vehicles traveling east on are all hot and the reflections from the underbodies of the vehicles can be seen in the lanes.....57

**Figure 34.** Citizens Area Transit (CAT) Bus. The engine location for the bus is in the rear of the vehicle. The bus is obviously hot, and the exhaust pipe location can be seen through the body of the bus.....57

**Figure 35.** Hot SUV. The reflection can be seen on the road, but the right edge of the reflection blends in with the road reflection.....58

**Figure 36.** Cold DRI employee vehicle. This vehicle is known to have been sitting long enough to reach the ambient temperature, however the high temperature and the driving time, approximately 20 seconds, from the parking lot to the road was enough for the vehicle to warm up noticeably.....58

**Figure 37A-C.** Hot vehicles with the image adjusted to see the reflection from the underbody of the vehicle without interference from the road reflection.....59

**Figure 38.** Hot truck. The truck in this image is hot. However the reflection from the underbody of the vehicle is masked by the emission from the road.....60

**Figure 39.** 2001 Hyundai Accent at cold start. Approximately 10 seconds from start.....62

<b>Figure 40.</b> Vehicle after driving around the parking lot one time. The tires and the exhaust system have warmed up and the reflection from under the vehicle can be seen on the road surface. Approximately 49 seconds after start.....	62
<b>Figure 41.</b> The vehicle is noticeably warmer than the previous figure. The reflection, the exhaust system, and the tire treads are brighter. This image was taken 39 seconds after Figure 40.....	63
<b>Figure 42.</b> The exhaust system of the vehicle is still increasing in brightness.....	63
<b>Figure 43.</b> The tailpipe of the vehicle is very noticeable; however the reflection does not appear to be getting any brighter.....	64
<b>Figure 44.</b> The tailpipe is the brightest object in the image, and the vehicle is fully warmed up. The reflection seems to have reached its brightest more than a minute previous to this image, but the tailpipe continued to get hotter.....	64
<b>Figure 45.</b> Results from Regis High School parking lot. The results include the data from all vehicles that were measured on two consecutive days.....	67
<b>Figure 46.</b> Cold start with 0.95 %CO.....	69
<b>Figure 47.</b> Cold start with low emissions. The %CO is 0.92.....	70
<b>Figure 48.</b> Cold start with 3.85 %CO.....	70
<b>Figure 49.</b> Cold start with high emissions. The %CO is 3.07. This vehicle would be classified as a repairable high emitter without the IR camera.....	71
<b>Figure 50.</b> Hot truck with 0.34 %CO.....	71
<b>Figure 51.</b> Graph of contrast ratio versus $1/T^4$ . As the road surface temperature increases, the contrast ratio decreases. The uncertainty bars are the standard deviation of the data.....	74

- Figure 52.** Typical graph of 200 seconds of the second by second (CO/CO<sub>2</sub>) data from FTP Bag 1 for a 1995 Jeep. The 90% recovery emissions are 0.067% CO, and the time to reach 90% recovery is 28 seconds.<sup>10</sup> .....76
- Figure 53.** Second by second data for a 1985 Chevy Spirit. This vehicle has high emissions when started, but decreases to an acceptable amount as the vehicle is driven. The amount of CO that is emitted is variable based on the driving cycle. The 90% recovery emissions are 0.42% CO and the time it took to reach 90% recovery was 144 seconds.<sup>10</sup> .....77
- Figure 54.** Graph showing warm up times derived from of the FTP data put into five MY bins, with the exception of 1977-1984, comparing 90% recovery warm up times vs. MY. The uncertainty bars are the standard errors of the mean. The data labels are the number of vehicles in each MY bin.....78

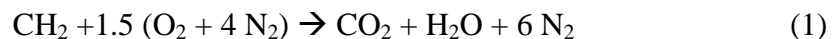
## List of Tables

- Table 1.** This table shows the number of vehicles that received a GOOD, FAIR, or POOR rating, as well as if the vehicle was a cold or hot vehicle. From the data of both days of measuring vehicles at the high school, there was only one vehicle received both a POOR rating and was a hot vehicle.....68
- Table 2.** This table gives the number of vehicles that received a GOOD, FAIR, and POOR rating, based on the %CO tailpipe emissions, at the time it took the vehicle to reach 90% recovery of the maximum emissions as well as the number of vehicles that received these ratings at the baseline emissions.....79

# Introduction

## Exhaust Chemistry

Motor vehicles are powered by the combustion of fuel, using the surrounding air as an oxidant. The air has a ratio of nitrogen to oxygen that is approximately 4:1 respectively, with other gases at much smaller concentrations compared to both oxygen and nitrogen.<sup>1</sup> Because nitrogen is the main component of air, it is also the main part of engine exhaust. The fuel of a gasoline engine is made of petroleum refined from crude oil that is blended with additives which perform many tasks, including to help the engine run smoothly.<sup>1</sup> Typical gasoline is mostly carbon and hydrogen, by weight, with percentages of roughly 86% to 14% respectively.<sup>1</sup> Using these approximations, the chemistry of a properly running stoichiometric gasoline fueled car is:



per one mole of carbon. Omitting water from consideration, the exhaust is approximately 14% carbon dioxide, leaving the rest of the emissions consisting of

nitrogen. For a perfectly running emission control system, one would expect these gases to come out the tailpipe with this ratio of  $\text{CO}_2 : \text{H}_2\text{O} : 6 \text{N}_2$ , with all of the oxygen from the air consumed in the combustion of the fuel.<sup>1</sup>

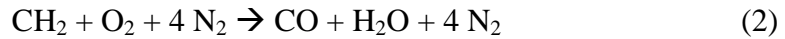
Vehicles typically do not convert fuel to  $\text{CO}_2$  and  $\text{H}_2\text{O}$  stoichiometrically, and therefore catalytic converters have been added to decrease the amount of CO (carbon monoxide), HC (unburned hydrocarbon), and NO (nitric oxide) being emitted due to incomplete fuel combustion.<sup>1</sup> For spark-ignition (SI) engines, the catalytic converter consists of an active catalytic material that allows for the gas to flow through and oxidize CO and HC and simultaneously carry out NO reduction. Three-way catalysts remove all three pollutants simultaneously. The active catalyst surface has a large surface area so that mass-transfer characteristics between the catalyst surface and the gas phase are sufficient to allow for close to 100% conversion. The active catalyst, typically platinum or palladium with rhodium for NO reduction, is finely dispersed on a cordierite extruded monolith.<sup>2</sup> The more expensive noble metals are used because they resist deterioration and have very good catalytic activity.<sup>2</sup>

In conjunction with the catalytic converter, an oxygen sensor (OS) is also used to maintain a stoichiometric air/fuel mixture.<sup>1</sup> There is one OS in the exhaust manifold, which provides rapid light-off of the sensor after start<sup>1</sup> to get the emissions under control quickly. The body of the OS is made of platinum coated  $\text{ZrO}_2$  ceramic<sup>2</sup> that is stabilized with  $\text{Y}_2\text{O}_3$  to ensure electrical conductivity at low temperatures.<sup>1</sup> It is mounted in the exhaust stream to monitor the oxygen

content of the ambient air and the oxygen in the exhaust stream. The OS provides a voltage to the engine that is dependent only on the oxygen concentration in the exhaust.<sup>1,2</sup> The signal gives the engine feedback and allows for the fuel intake to be controlled, letting more or less fuel in, to control the air/fuel ratio, thus giving a closed-loop operation.<sup>1</sup> Through feedback of the oxygen concentration based on a voltage from the OS output, the engine is able to adjust the air/fuel ratio depending on the voltage of the OS compared to a reference voltage.<sup>1</sup> If the OS voltage is lower, then the engine is running lean, and if the voltage is higher than the reference, then the engine is running rich.<sup>1</sup>

However, in real vehicles, the exhaust does not follow stoichiometry exactly. Vehicles will run either fuel rich or fuel lean depending on the engine operating mode. In a vehicle that is running fuel rich, there is more fuel in the combustion chamber than oxygen, and the fuel does not fully oxidize. The vehicle is programmed to run rich under the following circumstances: 1) starting the engine,<sup>3</sup> 2) when the oxygen sensor is broken<sup>3</sup>, and 3) under full power conditions.<sup>4</sup> This ensures that the engine starts when ambient temperature is cold and that the vehicle maintains its drivability during the warm-up of the vehicle.<sup>3</sup> This fuel rich mode on starting the vehicle adds extra fuel into the combustion chamber to ensure that there is a sufficient amount of fuel vapor to allow the spark to initiate a flame front and start the engine. This procedure adds unburned hydrocarbons (HC) into the exhaust emissions. If an engine is running fuel rich

and the engine is getting 33% less air, the chemistry of the exhaust changes to:



per mole of carbon.<sup>1</sup> All of the carbon is converted to carbon monoxide (CO), which is 20% of the emissions from the vehicle's tailpipe. There is no longer any conversion of carbon to carbon dioxide (CO<sub>2</sub>), even though there is only a small decrease in air to the combustion chamber.<sup>1</sup> This brief overview is a more extreme case than any on-road vehicle; however, observed CO/CO<sub>2</sub> ratios of 0.5 to 1.5 are not unusual. This is in fact a major over simplification of the combustion chemistry of a vehicle, but demonstrates how a decrease of the air/fuel ratio will affect the vehicle's emissions.<sup>1</sup> When the engine runs rich, unburned fuel is also emitted and hydrogen is formed via the water-gas shift reaction



Remote sensors correctly identify vehicles in a cold-start mode, which have no repairable fault, as relatively high emitters of pollution.<sup>5</sup> For this reason it is desirable in a "high emitter identification" program to remove cold cars from the data base. Infrared thermal imaging of automobiles has the potential to



determine if a car is hot or cold (i.e. a car that has just been started would be cold compared to a car that has been operating for several minutes.)<sup>6</sup> With a low-cost infrared camera, thermal images of numerous vehicles and their surroundings were taken to evaluate this potential.<sup>7</sup>

### Hot and Cold Vehicle Studies

Cold start emissions are defined as emissions from a vehicle with its engine and other vehicle components that are at ambient temperature. Hot stabilized emissions are from a vehicle whose engine and exhaust components are at temperatures higher than ambient temperature because of prolonged driving. In order to compare a vehicle's hot and cold emissions, the vehicle is driven using a standardized test cycle, such as the Federal Test Procedure (FTP), at cold start and when the emissions are stabilized at hot temperatures.<sup>8</sup> For certification testing, the test conditions must include a 74°-76°F soak time of twelve hours, however, a vehicle is rarely ever driven under these conditions year round. Therefore, the United States Environmental Protection Agency (USEPA) requires that the ability for the vehicle to start, as well as its drivability, not be compromised when the ambient temperatures are lower than test conditions.<sup>3</sup> When the ambient temperature is cold, the fuel in the combustion chamber does not vaporize quickly, thus there may not be enough fuel vapors to ignite when a spark occurs in the engine.<sup>6</sup> For this reason, more fuel is added to the combustion chamber, thus

increasing the fuel/air ratio. This ensures there is enough fuel vapor to have adequate start up and drivability when the vehicle is warming up.<sup>9</sup> The combination of increased fuel enrichment, poor combustion, and slow catalyst light-off results in a high concentration of HC and CO in the emissions.<sup>3</sup>

Cold start vehicles are known to have higher tailpipe emissions of HC and CO, from 4% to 88% higher,<sup>8</sup> due to the fuel rich operating mode and the fact that the exhaust after treatment system is too cold to be effective. In this engine mode, there is not enough air to fully burn all of the fuel and therefore any remaining fuel in the combustion chamber is released into the exhaust manifold. The vehicle is the coldest at the initial start, and because the engine temperature is related to the rate of fuel consumption, the fuel/air ratio is the richest at that moment and the most CO and unburned HC is released into the exhaust. The fuel/air ratio, CO, and unburned HC in the exhaust decrease as the vehicle temperature increases and reaches a closed loop operation for a properly running vehicle.<sup>3,10</sup>

During the 1970s, the FTP driving cycle of speed versus time was introduced by the USEPA to act as a certification test to measure the emissions from new vehicles.<sup>4</sup> The driving cycle was obtained from a driving survey taken in downtown Los Angeles, California in the 1960s, and is known as the LA-4.<sup>4</sup> This cycle simulates a vehicle driving 7.5 miles, including a cold start after a 12 hour soak time at 75°F, stabilized emissions, and a hot start after a 10 minute soak.<sup>4</sup> The full FTP includes a hot start portion of the FTP cycle that was added

in 1975, which makes the test about 11 miles long with an average speed of 21.2 mph.<sup>2</sup>

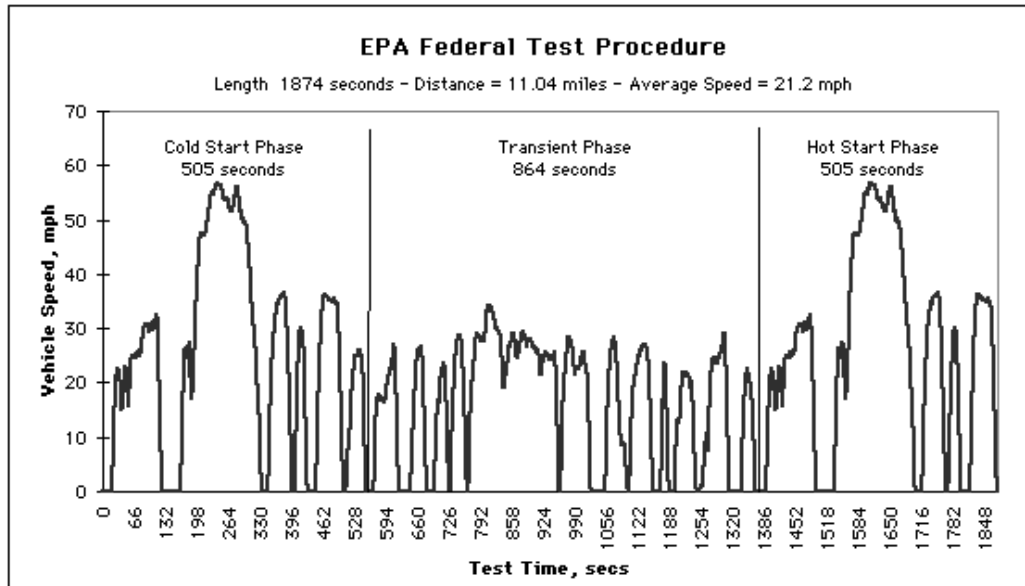


**Figure 1.** FTP Driving Cycle speed- time trace.<sup>11</sup> This trace of the FTP cycle does not include the ten minute soak time between the transient phase and the hot start phase.

The vehicle is put on a chassis dynamometer and the emissions are collected into bags via a constant volume sampling (CVS) dilution procedure for each portion of the test. Bag 1 includes the cold start emissions, Bag 2 represents the stabilized emissions, and Bag 3 includes the hot start emissions. Each bag is weighted a certain percentage and the average emissions are:

$$\text{Average Emissions} = 0.206(\text{Cold Start Phase}) + 0.521 (\text{Stabilized Phase}) + 0.273 (\text{Hot Start Phase}) \quad (4)$$

Because the FTP cycle was chosen as a downtown route, the maximum speed is 56 mph and a weighted average speed is 19.6 mph, it is not representative of urban driving. In real on road driving, the maximum speed is over 56 mph, and as the engine load increases, more fuel is required resulting in increased emissions.<sup>4</sup>

Because there are limitations in the FTP cycle, the USEPA phased in the US06 cycle (Figure 2) from 2000-2004 as part of vehicle certification. The cycle is also known as the supplemental FTP (SFTP), and is used in addition to the FTP to certify vehicles. The US06 tests the vehicle emissions control over a wider range of vehicle speeds and loads, but does not take the road grade into account. Therefore, while the required USEPA emission testing does not simulate real world driving, it does approximate harder driving conditions, including speeds above the legal driving speed.

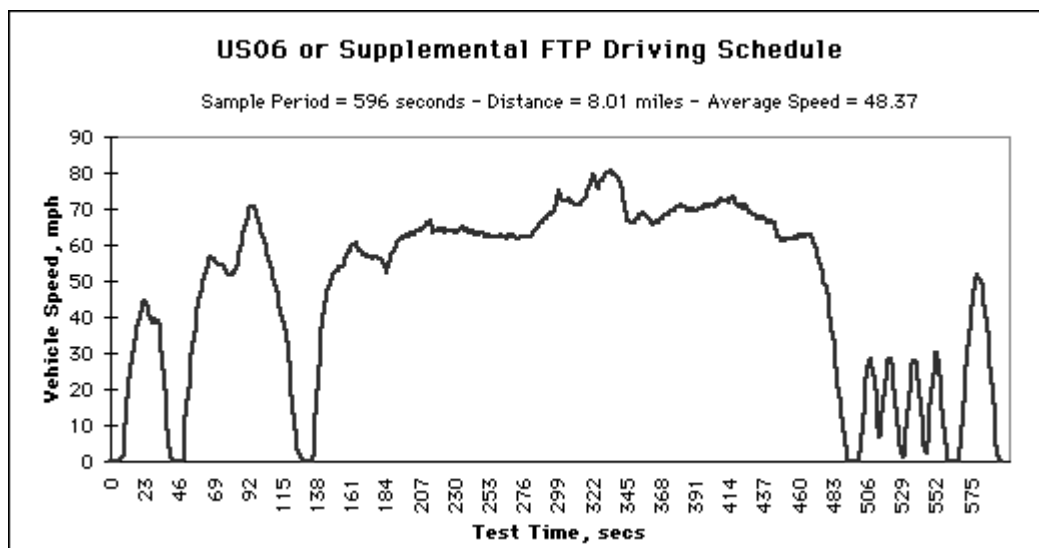


**Figure 2.** US06 Driving Cycle speed-time trace.<sup>11</sup>

The catalyst needs to be at a temperature above 250-300°C for it to be effective in converting CO and HC to CO<sub>2</sub> and H<sub>2</sub>O,<sup>1</sup> and the oxygen sensor must be above 250°C to operate correctly.<sup>3</sup> When oxygen sensor temperatures are below this range, the vehicle will not be working at or near stoichiometric combustion conditions, thus increasing the CO and HC in the exhaust. Above these temperatures the vehicle emissions should be stabilized and controlled within the limits for CO<sub>2</sub>, CO, HC, and NO<sub>x</sub>. However, if the vehicle has reached a temperature sufficient for catalyst light-off (the temperature at which the catalyst become more than 50% effective<sup>1</sup>) and is still a gross emitter of emissions, then the vehicle needs repair to control its emissions.

The oxygen sensor of the vehicle is one of the limiting factors in a vehicle controlling its emissions.<sup>12</sup> In order for vehicle manufacturers to obtain a quick light-off time and reduce the amount of unburned HC, Delphi Automotive Systems developed a fast “light-off” sensor in 2000.<sup>12</sup> This sensor allows for closed-loop, stoichiometric control of the emissions within 10 seconds, which is also before the first cycle acceleration of the FTP (see Figure 1). They were able to reduce HC emissions by 8.1% using a planar oxygen sensor and a shorter closed-loop time. The CO emissions were also reduced. The vehicle was adjusted to have the leanest possible start up air/fuel ratio without impacting the drivability of the vehicle.<sup>12</sup>

In a study sponsored by the American Association of State Highway and Transportation Officials, the Federal Highway Administration, conducted in the

National Cooperative Highway Research Program, and administered by the Transportation Research Board of the National Research Council, it has been observed that the time for a vehicle to reach catalyst light-off is decreasing with each newer model year (MY). The study was done by the Burns College of Engineering at the Center for Environmental Research and Technology (CE-CERT) by Theodore Younglove and his group. The study was a component of a four year research project to develop a Comprehensive Modal Emissions Model (CMEM). Sample vehicles were recruited from the on-road fleet, including California certified vehicles and 49-state vehicles. Each vehicle was tested using a complete 3-bag FTP test a high-speed cycle (US06), and a modal emission cycle (MEC01) developed by the research team.<sup>10</sup> Emissions were measured in the exhaust manifold “engine out” and after the catalyst “tailpipe out.” Engine out refers to the exhaust coming directly from the engine, and tailpipe out refers to the exhaust coming from the tailpipe. Real time data traces, in grams of pollutant, were obtained as well as the traditional bag data. The data were then used to determine light-off times and determine catalyst efficiency for the vehicles.

Figure 3 shows the catalyst light-off times versus model year of 241 in-use light duty vehicles in this study conducted by Younglove, et al.<sup>13</sup> Younglove, *et al.* calculated the catalyst light-off times by first determining the catalyst

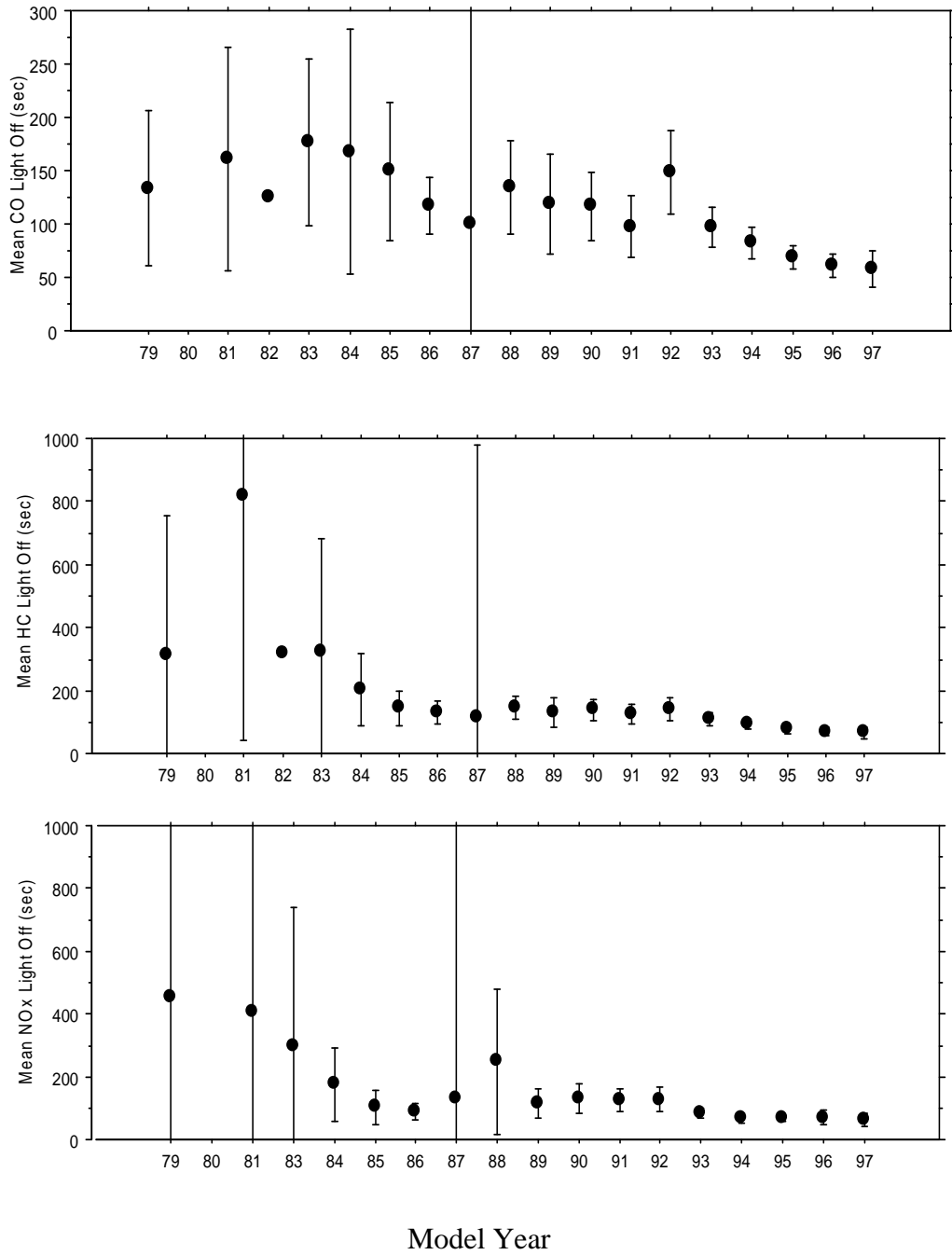


**Figure 3.** Mean catalyst light off time by model year for a) CO, b) HC, and c) NOx from Younglove *et al.*<sup>13</sup>

efficiency of each vehicle. They calculated the catalyst efficiency for FTP bag 1 and bag 2 using the following equations:

$$\text{Catalyst Efficiency (FTP bag1)} = \frac{\text{Out (FTP bag1)} - \text{Tail - Out (FTP bag 1)}}{\text{Engine - Out (FTP bag1)}} \quad (5a)$$

$$\text{Catalyst Efficiency (FTP bag2)} = \frac{\text{Out (FTP bag2)} - \text{Tail - Out (FTP bag 2)}}{\text{Engine - Out (FTP bag2)}} \quad (5b)$$

The Bag 2 catalyst efficiency was used to compare the cold start effects (Bag 1 only) to the hot-stabilized cycle. The catalyst light-off times were found by timing the vehicle from start to 50% of the catalyst efficiency. The light-off times observed by the Younglove group were dependent on driving cycle, and therefore they may not correlate with other driving cycles. The average light-off times were found from the efficiencies (equations 5a and 5b) and then plotted against model year for each pollutant, CO, HC and NOx. Large uncertainties caused by variability in light-off times for older model years are due to the inability of determining the status of the catalytic converter, as well as the small number of vehicles sampled per model year (MY).<sup>13</sup>

The soak time, the specified time allowed for a vehicle to cool, also has an effect on the initial emissions for a cold start based on FTP Bag 1 test conditions. Shorter soak times have a tendency to produce lower emissions and have a lower



fuel/air ratio.<sup>10</sup> As the soak time decreases, the vehicle does not have sufficient time to equilibrate to the ambient air temperature. Therefore the vehicle is not a “true” cold start. In order to be sure that the vehicle is a cold start, the temperature of the catalyst should be below the catalyst light-off temperature. If the soak time does not allow for this cooling, then the vehicle emissions should be that of a hot vehicle.

The large uncertainties in light-off times for older MY vehicles are due to both the small sample number and inconsistent light-off times.<sup>13</sup> Vehicles with MY newer than 1989 have small uncertainties due to consistent light-off times.<sup>13</sup> Younglove’s approach shows that 1996-1997 vehicles, the newest vehicles at the time of these tests, have consistent light off times of 40 – 80 seconds. Younglove also showed that, as expected, the light-off time tends to increase with increasing odometer mileage, and is independent of MY.

Due to the importance of cold starts to this project and the availability of a database from CE-CERT, their FTP data are later reinterpreted herein using a different approach. Overall, the trends from the new approach were very similar to the obtained results, but on average, the light-off times were shorter with the new method.

## Fuel Efficiency Automobile Test (FEAT)

The FEAT unit was developed in 1987 at the University of Denver as a way to measure the emissions of a vehicle in real time as the vehicle drove by the instrument. Prior to the invention of FEAT, a vehicle's emissions could only be determined by placing a probe into the tailpipe of the vehicle, where the emissions were then pumped into an instrument to determine the exhaust composition. Because the FEAT unit uses non-dispersive infrared spectroscopy (NDIR) to detect the tailpipe emissions of CO and HC and dispersive UV to detect NO, there is no tailpipe probe that needs to be attached to the vehicle. Instead, the vehicle

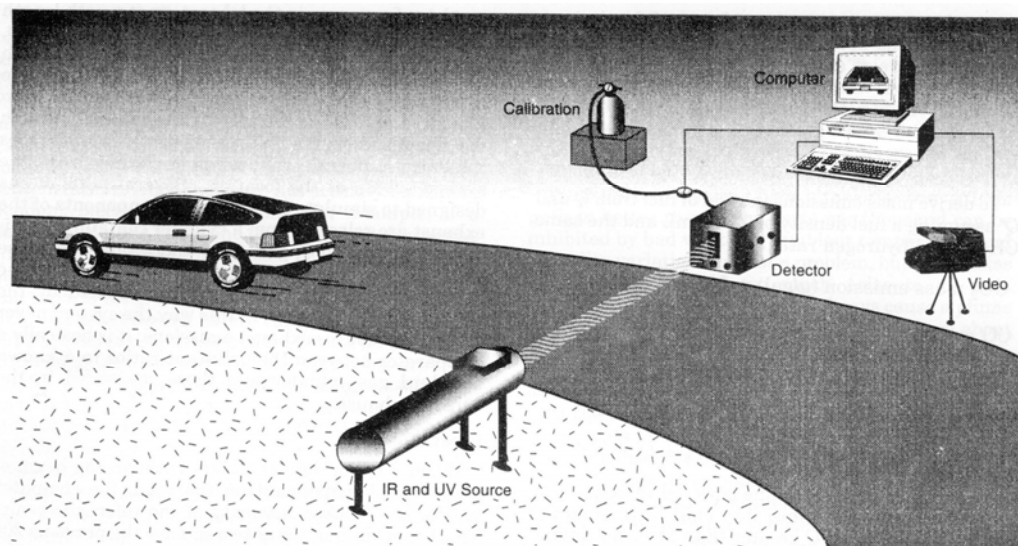


**Figure 4:** Typical layout of a remote sensing instrument observing vehicles across a single lane of traffic.<sup>14</sup>

drives past a beam of light that is pointed across the roadway at the FEAT unit which detects a decrease of light intensity as the vehicle's exhaust plume goes by. The FEAT unit uses absorption spectroscopy to determine the concentration of CO, HC, and NO, relative to the emissions of CO<sub>2</sub>.<sup>14</sup>

FEAT is only able to calculate ratios of CO, HC, and NO to CO<sub>2</sub> because the plume of emissions from the tailpipe of the vehicle can vary based on the wind and turbulence. The ratios of these exhaust components are constant for a given exhaust plume, Q for CO/CO<sub>2</sub>, Q' for HC/CO<sub>2</sub>, and Q'' for NO/CO<sub>2</sub>. On their own, Q and Q' are useful for describing the combustion system. When the combustion equations are solved using a more accurate formula for air, the vehicle operating conditions of the vehicle can be determined, including the instantaneous air/fuel ratio, %CO, %HC, and %NO, which can also be determined by a tailpipe probe as,

$$\%CO = \frac{42}{2.79 + 2Q + 0.42Q'} \quad (6a)$$

$$\%CO = Q (\%CO_2) \quad (6b)$$

$$\%HC = Q' (\%CO_2) \quad (6c)$$

$$\%NO = Q'' (\%CO_2) \quad (6d)$$

Because diesel and modern gasoline powered vehicles emit very little CO or HC, the Q and Q' are near zero.<sup>14</sup> In order for the Q value to be greater than zero, the engine must be running in a fuel rich mode. When the air/fuel ratio is increased,

either the vehicle is operating under a cold start mode, under power enrichment, or the vehicle is broken.<sup>14</sup> Most on road measurements in use today measure speed and acceleration so as to determine if a passing high emitting vehicle is under power enrichment conditions.<sup>15</sup>

For the purposes of providing public information at the Smart Sign,<sup>16</sup> GOOD, FAIR, and POOR were arbitrarily defined based on different concentrations of CO in the exhaust. If the vehicle has CO of less than 1.0%, the vehicle has GOOD emissions. Vehicles with CO emissions greater than 1.0% to less than 3.5% get a FAIR, and those vehicles that have CO emissions equal or greater than 3.5% CO or emit HC of greater than 2500 ppm as propane are rated as POOR.<sup>17</sup> The Smart Sign is located at the exit ramp from south I-25 to South Speer Boulevard where no cold start vehicles are expected to be present.

While the FEAT unit can detect the emissions from a vehicle, it cannot determine if the vehicle was a cold start or a broken vehicle with high emissions. Because cold starts do have higher emissions until the emissions control system is able to control them, the distinction between a hot and cold vehicle can be determined if the hot/cold status of the vehicle could easily be obtained. Stedman and Bishop have obtained a patent that involves an infrared camera to look at heat reflected from the underbody onto the road surface of the vehicle to determine the status of the emissions control system.<sup>6</sup> However, at the time of the patent the camera needed to be cooled with liquid nitrogen, was very expensive, and was not feasible for unmanned use.

## History of Infrared Radiation

Sir William Herschel first discovered infrared radiation in 1800 by accident. He was looking for a filter to reduce the brightness of the sun's image by testing different colored glass in telescopes, but found that some reduced the amount of heat that passed through. Herschel then set up Newton's prism experiment looking for the heating effect of the different color of light, not the visual distribution of light.<sup>7,18</sup> He used a blackened mercury thermometer and moved it slowly through the colors in the spectrum and noticed that the temperature increases as the thermometer moved from violet to red light. Herschel expected these results because Landriani had done this same experiment in 1777, and he had observed the same effect. However, Herschel was the first to realize that the maximum temperature did not lie in the visible spectrum. He called the maximum heat beyond the red region of the spectrum the "radiant heat," and wrote two papers on the subject.<sup>18</sup> He continued to move the thermometer into the dark region beyond the obvious light, and found the maximum well beyond the red region of the visible spectrum. He called this region the thermometrical spectrum.<sup>7,18</sup> This region was later called the infrared spectrum.<sup>6</sup>

Until 1829, thermometers were the only method of detecting infrared radiation, when Nobili invented the thermocouple. In 1835, Ampere was able to use the thermocouple to demonstrate that the infrared region has the same optical

characteristics as visible light.<sup>18</sup> Melloni connected several thermocouples together to create a thermopile, which was 40 times better than the best thermometers of the day. It was sensitive enough to detect the heat from a person standing three meters away. Eleven years later, the son of William Herschel, Sir John Herschel, created the first thermal image. The image was produced from the differential evaporation of a thin film of oil. This resulted in interference patterns in the reflected light that could be seen by the eye. He called this a “heat-picture.” The image could then be primitively recorded on paper, which he named a “thermograph.”<sup>7</sup>

The invention of the bolometer in 1880 made huge improvements in infrared detection. The original bolometer was made of a blackened strip of platinum connected to a bridge circuit onto which infrared radiation was focused and a galvanometer responded. It was said to be able to detect a cow 400 meters away.<sup>7</sup> The bolometer was sensitive to small changes in radiant heat to one hundred-thousandth of a degree Celsius (0.00001°C).<sup>19</sup>

In the early 1900s, the infrared region was investigated thoroughly, and many patents were issued for devices to detect personnel, artillery, ships, aircraft, and icebergs. Military programs researched systems that could be used for enemy intrusion, remote temperature sensing, and “flying torpedo” guidance. Much of the research on infrared imaging was conducted during this time, but was not available until the mid-1950’s when a military secrecy ban was lifted. Soon afterwards the technology became available for civilian use.<sup>7</sup>

## Blackbody Radiation

There are many types of radiation which are broken up into different categories based on the frequency of the radiation, from radio waves with the lowest frequency, to gamma rays which have the highest frequency.<sup>20</sup> A blackbody is an object that is capable of emitting and absorbing all frequencies of radiation uniformly.<sup>21</sup> A good approximation of a blackbody is the emission from a pinhole in an empty container that is held at constant temperature.<sup>20,21</sup> The radiation that is able to escape from the pinhole has bounced off of the inside walls, and has therefore come to thermal equilibrium with the walls.<sup>20,21</sup> As the

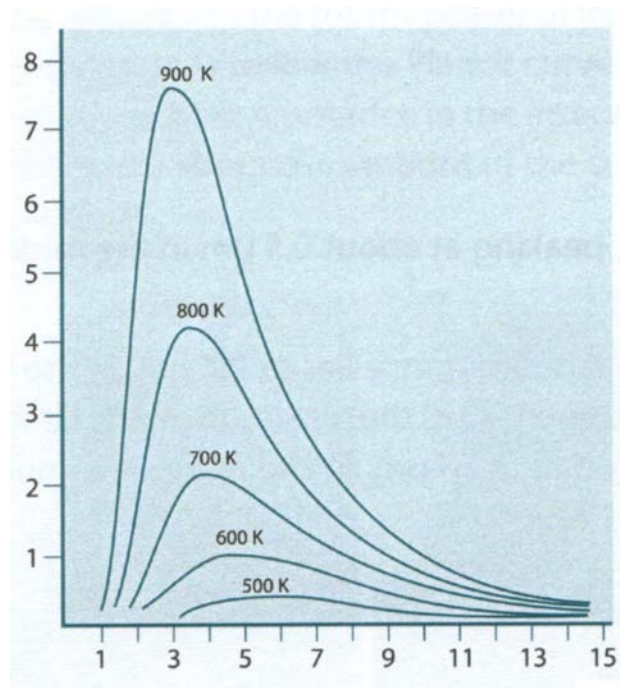


**Figure 5.** Blackbody radiation curves. The x-axis is the wavelength in  $\mu\text{m}$ , and the y-axis is the spectral radiant emittance ( $\text{W}/\text{m}^2 \times \text{nm}$ ).<sup>7</sup>

temperature is raised, the energy distribution shifts towards the visible region, and the color that is perceived shifts towards the blue, as in Figure 5. The maximum wavelength of a blackbody can be determined by using the Wien Displacement law,

$$\lambda_{\max} = \frac{1.44}{5T} = \frac{0.588}{T} \quad (7)^{21}$$

where the  $\lambda_{\max}$  is the wavelength, in cm, which corresponds to the maximum of the distribution at temperature T (K).<sup>21</sup> For the peak at 900K in Figure 5, the  $\lambda_{\max}$  is 3200 nm. The total energy density of the radiation is proportional to  $T^4$ :

$$E = \alpha T^4 \quad (8)$$

which is known as Stefan's Law and was discovered in 1879.<sup>21</sup>

For temperatures that are typically measured by the infrared camera on road surfaces, such as 273K, the  $\lambda_{\max}$  is 10.5  $\mu\text{m}$ , while at 313K, typical road temperature in Las Vegas, the  $\lambda_{\max}$  is 9.4  $\mu\text{m}$ . These maximum wavelengths are well within the 7.5 – 13  $\mu\text{m}$  ( $1300\text{-}700\text{ cm}^{-1}$ ) temperature range of a commercially available infrared camera.

Max Planck developed a theory that agreed with the experimental blackbody curves, and accounted for the ultraviolet catastrophe. In order for his



theory to work, Planck assumed that the radiant energy emitted by a collection of oscillators, atoms and molecules, in the blackbody could only emit radiation in quantized amounts of  $h\nu$ , where  $h$  is Planck's constant ( $h = 6.626 \times 10^{-34} \text{ J}\cdot\text{s}$ ).<sup>20</sup>

$$E = nh\nu \quad n=0,1,2\dots \quad (9)^{19}$$

Figure 6 illustrates the Planck distribution.

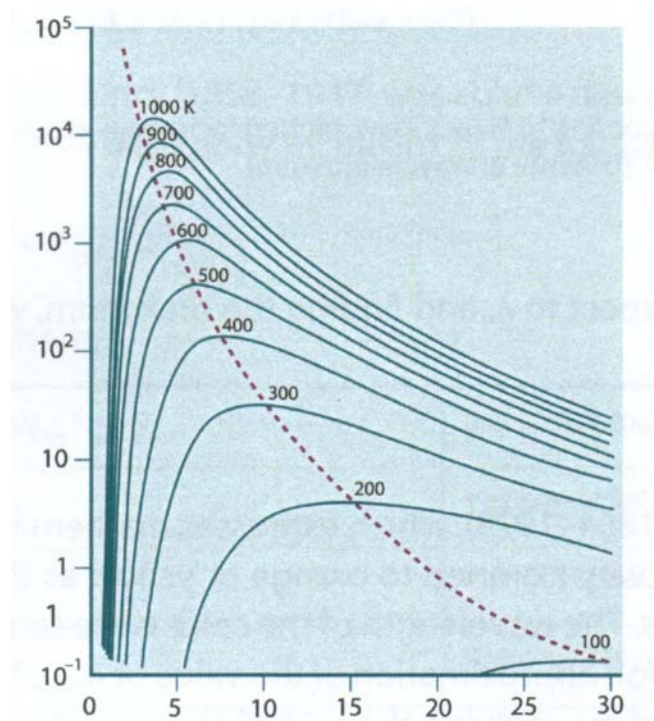


**Figure 6.** Planck Distribution. The x-axis is the wavelength in  $\mu\text{m}$ , and the y-axis is the spectral radiant emittance ( $\text{W/m}^2 \times \mu\text{m}$ ).<sup>7</sup>

# Experimental

## Infrared Camera

All of the experiments that were done used an infrared camera from FLIR Systems, North Billerica, MA. The camera used is a FLIR ThermoVision™ A20V camera with a FireWire configuration. The camera is equipped with a field of view (FOV) of 25° and a vanadium oxide focal point array uncooled microbolometer. The camera's infrared (IR) spectral range is 7.5-13 μm. The range of operating temperatures for the camera is -15° – 50°C (5 – 122°F).<sup>7</sup> Infrared cameras measure total radiance. Some are equipped with software which attempts to derive temperature of objects in the FOV from the irradiance readings; however, this depends on knowledge of the unknown emissivity. Since the emissivity varies based on the material that each object is made of, the images are analyzed from the true raw data, and not from a derived temperature.

## Thermal Image Set-up

The camera is turned on by inserting the power cord into the back of the camera and hooking up to a monitor to view the images. The initial screen consists of a frozen image of squares that show a scale of colors. To get to the

camera mode, the FRZ, Figure 7, button is depressed, and then an IR image of what is in the FOV is available. Upon pushing the YES button, a menu pops up onto the monitor, which allows the user to select different options. The “Image” menu is highlighted by using the up and down arrows. Once highlighted, the YES button is pressed, and another menu of “Image settings” will appear. The arrow keys are used to navigate between the different menu selections. To change the color scale to black and white, the box next to “Palate” is highlighted and the left or right arrow keys are used to change the palate to “Gray (white hot).” The down arrow is then pressed once to highlight the “Auto adjust” box and the left or right arrow buttons are used to turn the auto adjust off. Once these settings are chosen, the YES button is pressed again and the menu will disappear, and a box will then be displayed in the upper left corner that says “Manual.” The manual setting is used to keep the camera from self-adjusting to the surroundings. The gray scale is used for ease of interpreting the images from the camera. It allows those who are colorblind to see the same information as those who are not colorblind.

The IR scale for the level and span is set by holding the SEL button for more than a second while the camera observes a known hot vehicle with colder objects in the FOV. Then the camera is focused by using the manual focus adjust ring at the front of the lens. The hottest object is now white, and the coldest object is shown as a black object. In order to change the level and span of the

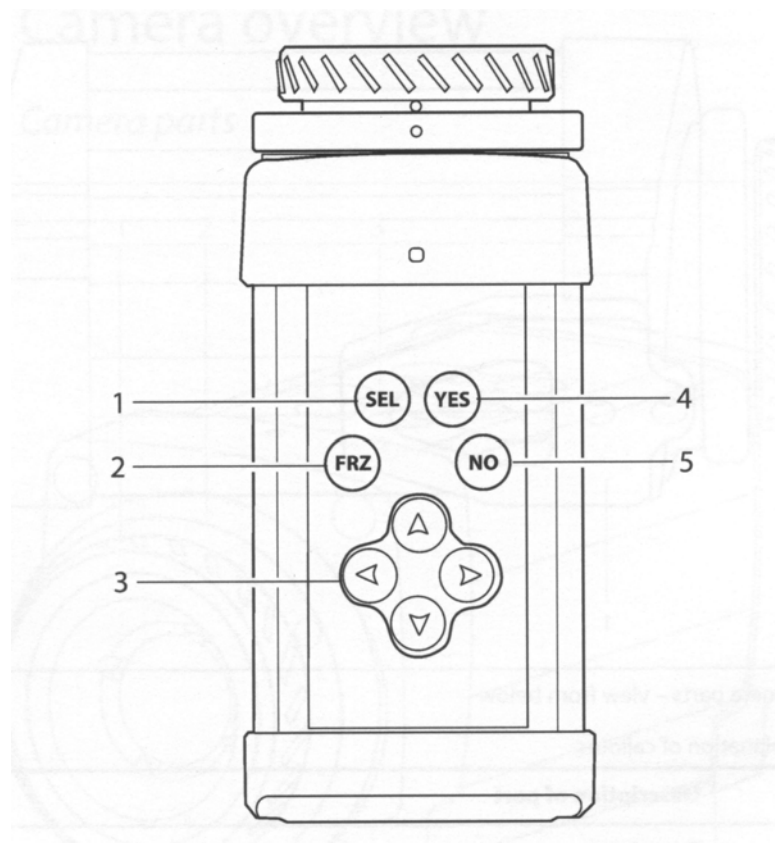


**Figure 7.** Schematic diagram of the top of the FLIR camera. 1) SEL Button, used to adjust the camera scale in manual mode. 2) FRZ Button, used to start the camera mode and can be used to freeze an image on the screen and can save images to the camera when pressed for longer than a second. 3) Navigation Pad, used to navigate the menu options. 4) YES Button, used to display the menu, a menu option. 5) NO Button, used to unfreeze an image, leave menu options.<sup>7</sup>

camera, the SEL button is held down while any of the arrow buttons are depressed. These parameters can be likened to brightness and contrast respectively. The average level is changed using the up and down arrows, while the span is changed using the left and right arrows. If the original “hot” vehicle was showing very hot exhaust system components, the level needs to be lowered using the down arrow and the span decreased using the left arrow. This will then optimize the visibility of the infrared reflection.

### On-Road Set-up

The FLIR A20V camera is set-up similarly for all experiments. The camera is plugged into a power source and connected to a monitor and a VCR. The image is set to a black and white color scale, in which the hottest object in the FOV is shown as white. The focus ring on the lens focuses the image in the FOV. The camera is then aimed at either the side or the rear of vehicles in order to get a thermal image of each vehicle and determine if it is a cold start or a hot vehicle.

The VCR can be attached directly to the camera or through the FEAT unit, which will freeze an image after a vehicle has driven past the instrument, blocking and unblocking the light source. The FEAT unit also superimposes the percentages of CO, HC, and CO<sub>2</sub> onto the frozen image. When the camera is connected directly to the VCR, the image that is recorded is a streaming infrared video image without emissions information.

## Road Surface Temperature

The temperature of the road surface was obtained using a Raytek Minitemp MT4. It is a battery powered infrared thermometer with a laser sighting beam. The thermometer has a temperature range of  $-18^{\circ}$  to  $+260^{\circ}\text{C}$ , with a response time of 500 msec. The thermometer assumes an emissivity of 0.95. The thermometer was not acquired until December of 2003; therefore, in the initial experiments the road temperatures were estimated from ambient data.

## Initial Experiments

The camera, a VCR, and monitor were set up on Iliff Ave. on a sidewalk north of the Olin Building at the University of Denver using a Honda gasoline generator for power. The sidewalk is across from a parking garage that holds mostly student vehicles from the nearby dorms, and it was assumed that most of the vehicles that left the parking garage would be cold, while the vehicles entering the lot would be hot. The Iliff Ave. experiments were done to determine if differences between hot and cold vehicles could be seen. The first time the camera was set-up on 29 August 2003, it was set in the auto mode and in the “Iron” color scale. This is the initial mode that the camera was shipped in, and in order to be more familiar with the camera and the images that the camera produced, these were the initial set-up conditions. It was then decided that the camera should be set to the manual mode in order for the operator to fix the range

of the camera as well as to be in a black and white scale to allow for easier interpretation of the images. Therefore, all subsequent experiments were set up in the manner described above. The change was made in order to ensure consistency in future measurements.

At this location, the camera was set up to look at the side of the vehicles. Because the reflection from under the vehicle is more important than the fine details of the vehicle, the camera does not need to be clearly focused on the car. If the vehicle is hot, the diffuse reflected heat from the underbody of the vehicle should be apparent, even if the camera is not focused very well.

The purpose of the next set of experiments was to study a wide range of road conditions to determine the limitations of the camera, and to test the applicability of the chosen operating mode for this application.

### Cold Road Conditions

The infrared camera was set-up on 10 September 2003 with a VCR and monitor, all powered by a Honda generator on the sidewalk just south of Cherrington Hall on the University of Denver campus near an employee parking lot when the outside temperature was approximately 36°F. The road temperature was not taken; however, the road was at least the ambient temperature or lower due to the cloudy weather conditions as well as the time of day. The camera was set up in the late afternoon in order to observe the vehicles leaving the university.

The lot was chosen because a high volume of vehicles leave at the end of the work day, and would have had sufficient amount of time to cool to the ambient temperature. The road surface was the coldest feature in the FOV, and the span was over a wide infrared range.

### Hot Road Conditions

In order to study the effects of hot road surfaces, temperatures greater than 100°F, the camera was set up in Las Vegas, NV on 05 May 2004. The camera was set up outside of the Desert Research Institute (DRI) research building facing eastbound on Flamingo Road. Extension cords were used to get power to the camera and the camera was plugged into a VCR to videotape the vehicles as they drove by. Approximately every thirty minutes, the temperature of the road surface was measured using the infrared thermometer.

The set-up for the camera was slightly different than under other road conditions. At ambient temperatures approaching 90°F, as well as sunny skies, the road surfaces approach temperatures of 140°F. The level of the camera was set to allow for the very small difference in infrared intensity between the road surface and the heat reflected from the vehicles onto the road surface by adjusting the image to decrease the brightness. The level of the image needs to be adjusted so that the road is darker. This will darken the entire image, but will allow the



slight differences in the reflected heat from the vehicle and the heat from the road surface to be seen.



**Figure 8.** Camera set-up on Flamingo Road in Las Vegas, Nevada.

### Hot Road Cold Start

A 2001 Hyundai Accent that had been sitting in the DRI parking lot since 9:00 am, was assumed to have reached the ambient temperature outside by 1:00 pm. The vehicle was driven around the parking lot at the DRI to see what a cold

start vehicle would look like under very hot road conditions. The camera was set up with a VCR and monitor, powered by a battery supplied by DRI. The vehicle was then driven past the camera repeatedly for several minutes to allow enough time for the vehicle to warm up. This exercise produced a series of images which show a vehicle from a cold start to hot that were used for later analysis.



**Figure 9.** Set-up in DRI parking lot for observing the cold start vehicle warming up as it was driven around the parking lot.

## FEAT Set-Up

The infrared camera was set up in conjunction with the FEAT 3000 instrument in order to confirm that the difference between hot high emitter and cold high emitters could be determined. The instrument was set-up under normal conditions, as can be seen in Figure 10. The infrared camera was positioned in the same place as the camera in the set-up schematic. The computer was programmed to freeze an image when the light beam of the source was unblocked after >40 ms block. The date, time, and percents of CO, CO<sub>2</sub>, and HC that are emitted from each vehicle are superimposed on the frozen image of that vehicle.

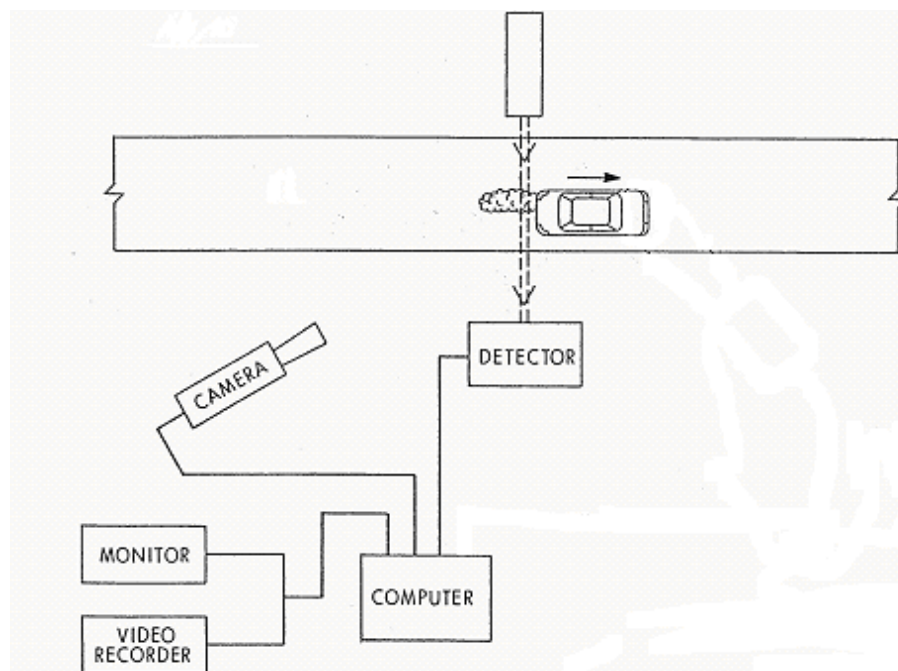


**Figure 10.** Schematic drawing of FEAT unit and the infrared camera set-up.<sup>6</sup>

## Cold Start with FEAT

On several occasions, the FEAT unit was set up in the Seely G. Mudd building parking lot at the University of Denver on 15 January 2003. A 1986 Chevrolet Celebrity station wagon, named Blue by the Phillipson Research Group as, was known to have been sitting in the parking lot overnight and was used for this study. The vehicle was driven around the parking lot to watch the vehicle warm up and see the emissions decrease. A FEAT 3000 unit was set up to measure CO, CO<sub>2</sub>, HC and NO as the vehicle drove past the instrument.

## Regis High School Study

The FEAT 3000 unit was taken with the IR camera to Regis Jesuit High School on two consecutive afternoons in December of 2003 to compare the IR image of the vehicles leaving the school campus, after classes were dismissed, to the emission readings from the FEAT 3000. This location was chosen because most of the measured vehicles had been sitting for approximately 6 hours, and was known cold start vehicles. It was anticipated that there would also be several warm vehicles driven by parents that were entering the parking lot to pick up their children. The FEAT unit was set up to take emission readings for CO, HC, and CO<sub>2</sub>. The combination of the IR camera and the FEAT unit was used to test if cold vehicles that are high emitters of CO could be correctly identified by looking at the thermal image. The set up of the FEAT unit and the instrument was similar

to the schematic drawing in Figure 10. The source for the FEAT unit was set up across the street from the detector. The system was programmed to be triggered by a vehicle driving by and then superimpose the emissions reading on a still image of the vehicle. The still images were continuously recorded, which allows for later review of the IR image of each vehicle, as well as the emissions readings that the vehicle received. From these images and emissions readings, the Smart Sign rating of GOOD, FAIR, or POOR can be assigned, as well as if the vehicle was hot or cold.

In the future, the thermal image will be used in conjunction with the use of a normal video camera to get license plate numbers. The goal is to use both cameras in tandem to identify vehicles that are broken high emitters so that they can be ticketed by law enforcement. In the process of ticketing broken high emitters, law enforcement wants to avoid sending citations to the owners of high emitting vehicles that have no repairable fault, i.e. cold vehicles with higher emissions.

A similar experiment was also done at the University of Denver in the Seely G. Mudd building parking lot. The only difference in the two experiments was that CO, HC, NO, and CO<sub>2</sub> were measured. A vehicle that was known to have a cold engine was driven around the parking lot for several minutes to get emissions readings, as well as to determine the length of time needed for it to become warm enough for the emissions control system to begin functioning properly.



(A)



(B)

**Figure 11.** Pictures of the FEAT set-up at Regis High School. (A) Looking north at the source. (B) looking east along the access road towards the school.

## Analysis of the Infrared Images

The infrared images were recorded from an analog VCR tape to digital images by using Asus Image capture hardware, and the images were saved as JPEG files. Once the images were converted to digital images, the files were opened using Adobe Photoshop<sup>®</sup> CS. The “Info” tab on the right navigation panel is selected and the color readouts are changed to grayscale and the “Mouse Coordinates” is set to pixels. This allows for only one pixel to be read at a time, as well as have only one color variable. When pixels are boxed off, the histogram gives information about the selected pixels, such as the mean, standard deviation, median and the number of pixels that are selected.

The mean reported intensity reflected from the underbody of the vehicle and the road surface is determined by selecting a group of pixels in the reflected heat from the underbody of the vehicle and selecting pixels from the road as close to the vehicle as possible. The mean from the selected pixel group is recorded from the histogram. The contrast of the reflected infrared from the underbody of the vehicle and the emitted infrared from the road surface can be determined as a contrast ratio:

$$Ratio = \frac{R + E}{E} = \frac{R}{E} + 1$$

$$E = \text{Emission Intensity} \quad R = \text{Reflected Intensity} \quad (10)$$

It can be assumed that E is proportional to  $T^4$  from Stefan's Law on page 19, and therefore:

$$Ratio = \frac{R^*}{T^4} + 1 \quad (11)$$

$R^*$  includes the proportionality factors relating pixel intensity to absolute temperature. A graph of the ratio versus  $1/T^4$  can then be plotted to investigate the extent to which the observed trend in contrast ratio with temperature is predicted by equation 10.

### Reanalysis of the CE-CERT FTP Data

Due to the importance of cold starts to this project and the availability of a database from CE-CERT, the FTP data are reinterpreted here using a different approach. The data were obtained from CE-CERT on a CD with second by second emissions data for 348 vehicles. The data set included some vehicles without a catalyst, which were not included in this data analysis. The FTP vehicle Bag 1 data were plotted as a function of  $(CO/CO_2)$  versus time for each of the vehicles. The resulting graph was then used to determine 90% of the stabilized reading of a steady baseline emissions recovery, i.e. the time it took for the vehicle emissions to return from the maximum to within 90%, for each vehicle in



the data set. To get the emissions recovery, the maximum emissions and the baseline emissions were determined from the graph. Once those values were known, the 90% recovery emissions could be found using the following equation:

$$90\% \text{RecoveryEmissions} = \left( \frac{\text{BaselineEmissions} - \text{MaximumPeak}}{10} \right) + \text{BaselineEmissions} \quad (12)$$

Once the 90% recovery emissions were found, the time that it took the vehicle to reach that percent of CO emissions was determined from the graph. The time was then plotted against the MY of the vehicle with the other vehicles in the data set. The average times for five year bins of vehicles to reach 90% recovery was also determined.

## **Results and Discussion**

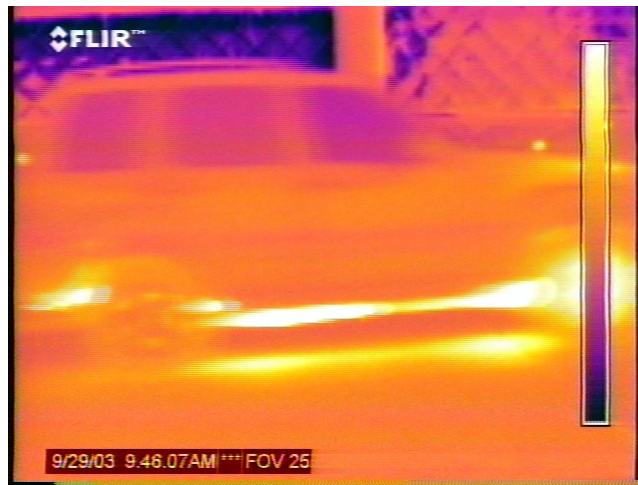
### **Initial camera set-up**

The initial set-up of the IR camera was on a sidewalk on the north side of Olin Hall looking at the traffic on East Iliff Avenue. The camera was set-up using the factory settings on the camera, which had the color palate set to “Iron” and the auto adjust on. For this color palate, black is the coldest object and white is the hottest object with purple, fuchsia, and yellow in between, such that the darker colors were for colder objects and the lighter colors for hotter objects. When an object enters the FOV of the camera it readjusts the image so that the coldest object in the image is black and the hottest object is white and that all of the objects of intermediate temperatures are scaled in between. The camera sometimes overcompensates when adjusting the temperature scale, and the image will darken and brighten as the camera adjusts until it reaches its level.

Although the auto adjustment does not affect the overall information of the picture, it may affect the images of vehicles that do drive past the camera in



(A) Initial vehicle driving past the camera.



(B) Vehicle following the initial vehicle in quick succession, with its image much darker due to the auto adjust mode on the camera.



(C) Darker image due to the camera's auto adjust mode.



(D) Camera still adjusting the image.



(E) The camera is no longer adjusting the scale of the image.

**Figure 12 A-E.** Infrared images using the Iron palate with the auto adjust on. After the first vehicle passes in front of the camera the image darkens and takes several seconds to adjust back to the same scale as the first image.

quick succession, as shown in Figure 12. In Figure 12b, the tires of the vehicle are hard to discern from the road surface, however it is not possible to determine if one would be able to see more detail from the image if the camera were not in the auto adjust mode. In the following figures, it can easily be seen that the brightness of the image decreases after the first vehicle drives past the camera. After 5 seconds, another vehicle has passed by the camera, however the camera has not finished adjusting the level of the image. The four following figures show the camera returning to an equilibrium level.

Although the “Iron” palate is colorful, as well as fun to look at, it could be difficult for someone who is colorblind to easily interpret the image. Also, the camera takes several seconds to adjust to the change in intensities of infrared

radiation after a vehicle has driven past. This can affect the level or the “brightness” of the image if several vehicles drive past the camera in quick succession. It was decided that the camera should be set to a palette that is easy to interpret, and the gray scale was chosen. The option of white as the hottest object in the image was chosen for its intuitiveness. Also the camera was set to the “manual” mode in order to keep the images from fluctuating in brightness.

The next step in obtaining infrared images from the camera was to use the manual mode and gray scale on the camera. These images in Figures 13 and 14 are also from the north sidewalk of Olin Hall on Iliff Avenue on 10 September 2003. While the images are a bit blurry, all of the necessary information can be seen in the image. The reflection from the underbody of the vehicle can still be seen, however the scale of the images is not optimal. The camera could have been adjusted to make the road surface a darker feature to show more contrast between the road and the reflected heat from the underbody of the vehicle.

The images from 29 August 2003 and 10 September 2003 (Figures 12-14) are taken from the side of the vehicle, which has the limitation of the vehicle being in the FOV for a very short time. While this set-up had convenient location and was a good starting point for learning how to use the camera, it would be beneficial to look at the vehicles from behind. This allows for the vehicle to be in the FOV for a longer period of time as well as to get a good view of the tire treads on the vehicle. It was also learned from a subsequent experiment that the tire treads heat up noticeably from driving on the road.



**Figure 13.** Hot vehicle driving east on Iliff Avenue. There is a bright reflection from the underbody of the vehicle, but the tire treads cannot be seen to further determine the status of the vehicle.



**Figure 14.** Hot vehicle. This vehicle has both a bright reflection from the underbody of the vehicle as well as warm side walls on the tires.

While adjusting the camera in the manual mode, it was learned that focusing the camera on sunny days can be somewhat difficult due to the sun glare on the monitor. The sun glare can also make it difficult to adjust the scale of the camera, and therefore a shield over the monitor could help to alleviate this issue.

### Cold Start Images

On 15 January 2003, the IR camera was set-up in conjunction with a FEAT 3000 unit in the S. G. Mudd parking lot. The camera was set up in the morning, and the sun was still behind the S. G. Mudd building, and for that reason the image of Figure 15 is very dark compared to the rest of the images of the Chevrolet Celebrity, affectionately named Blue.



**Figure 15.** Cold start of Blue. The %CO is 5.66, which is a high reading for a vehicle.



As Blue is driven around the parking lot, the emissions of CO are decreasing as the reflection of the underbody of the vehicle is increasing in brightness. The images in Figures 15-19 are typical of vehicles at cold start. As the vehicles are driven, the tire treads get warmer and in the IR image, they get brighter. The exhaust of the vehicle also warms up and the IR emission increases. The tailpipe emissions are also decreasing as a function of the vehicle warming up.



**Figure 16.** Blue shortly after cold start. The %CO at the time of start was 2.83. The image is darker than the following images because the camera was adjusted in between images.



**Figure 17.** Blue, with %CO of 2.07. The reflection from the underbody of the vehicle is much stronger than the previous figure.



**Figure 18.** Blue with 0.13 %CO. The vehicle has a much stronger reflection from the underbody of the vehicle, as well as a very bright exhaust system. The vehicle's emissions are now low enough to pass an emissions test. Blue took 224 seconds to warm up.



**Figure 19.** Blue with 0.13 %CO. The vehicle would still pass an emissions test, but is still warming up.



**Figure 20.** The vehicle is still emitting a constant percentage of CO in the exhaust, and is now fully warmed up.

## Images on Cold Road Surfaces

On 11 November 2003 (Figures 21-27), the camera was set up outside Cherrington Hall on the east sidewalk, facing south towards the parking lot exit. The outside temperature dropped from 36°F to 25°F in two hours. The actual road temperature of the road is not known. This particular study prompted the purchase of the infrared thermometer to measure the road temperature. Because the road surface was the coldest thing in the image, it is the darkest feature in the image. Only the sky is darker due to its transparency in the IR. Overall, the entire image is much darker than the previous images which were taken on warmer days.

It was assumed that all of the vehicles leaving the parking lot have been sitting long enough to cool down to ambient temperature, however when they left the parking lot they appeared to be hot. This is because when the vehicle is started, it warms up enough for the camera to detect the difference. The scale of temperatures that the camera sees is much smaller than the warmer days that the camera was taken out into the field. The road surface is cold enough that a small rise in temperature from the underbody of the vehicle can be seen, and therefore, even if the vehicle has not warmed up sufficiently enough for the oxygen sensor to be working, it may look like a hot vehicle based on the reflection of the vehicle. A cold start vehicle on cold days will have a reflection from the underbody of the vehicle, but it is not as intense as the reflection of vehicles that have been running

long enough for the oxygen sensor to run at closed loop operation. The tires on cold start vehicles also are not very warm. As a vehicle drives, it causes the treads of the vehicle to become warmer, and in an infrared image appear to be brighter. This effect can be seen in Figures 15 – 19, as Blue is warming up.

When the outside temperature is cold, as in the winter, the road surface is much colder than a car that has just been started, and therefore small changes in engine temperature are seen as reflections off the cold road surface. Thus, in the winter, an automobile will look hot much faster than it would on a mild day.



**Figure 21.** Cold vehicle. This vehicle is leaving the restricted parking lot across from the north side of Olin Hall, and has no bright underbody reflection or hot tire treads.



**Figure 22.** Cold start vehicle. This SUV has a very faint reflection from the underbody of the vehicle and the tire treads do not emit very much infrared radiation.



**Figure 23.** Cold start vehicle. This vehicle is leaving the metered visitor parking lot (304) across from Cherrington Hall, and the exhaust of the vehicle appears to be hot due to the small increase of heat from the vehicle starting. This vehicle has no strong reflection from the underbody of the vehicle or hot tire treads to indicate that it is warm.



**Figure 24.** Warm vehicle. It is unknown if the vehicle is fully warm. If the emissions for this vehicle were known, then the status of the vehicle could then be decided.



**Figure 25.** Hot truck. Has a very bright reflection under the vehicle as well as uniformly heated tire treads and sidewalls on the tires.





**Figure 26.** Hot Sport Utility Vehicle. This vehicle has both hot tire treads as well as a very bright reflection from the underbody of the vehicle.



**Figure 27.** Hot truck. The truck in this image has both hot tire treads and a bright reflection from the underbody of the vehicle. The reflection can be seen at a distance as long as the road surface is level.



## Effects of Snow on Road Surfaces

On a dry road surface, the heat from the underbody of the vehicle is reflected, and the hot/cold status appears readily detectable. This study was intended to determine how various road surfaces reflect infrared radiation. It was suspected that snow absorbs most of the infrared radiation that would otherwise be reflected by the road. While snow is a mostly absorbing surface in the infrared, liquid water is very reflective in the infrared. In addition, tire treads are also cooled in the snow, and therefore would not emit higher IR and appear to be cold, even if the vehicle had been driving around.

The first image which confirmed his hypothesis was of the Breckenridge Ski Area patrol SUV. This vehicle had been driven all day, but showed very little reflection on the snow covered parking lot surface, as can be seen in Figure 28. The tire treads are cold from driving on the snow, however, the sidewalls of the tires appear to retain some heat from driving around the resort.

Vehicles that are sitting in the sun will have bright areas on the body and the tires depending on where the sun hits the vehicle, which can be seen in the parked vehicles on the far left in Figures 28-31. As the vehicle drives around, and the sun hits the vehicle evenly, then the bright areas are not as apparent. These bright parts appear in the pictures from the Breckenridge parking lot, as well as in other areas that the camera was set-up. On cloudy days, these parts do not appear; such as in the images from the cold road study.



**Figure 28.** Breckenridge Ski Patrol SUV. The vehicle is hot, as can be seen by the hot engine through the grille, however because snow does not reflect IR radiation, there is no reflection on the road from the underbody of the vehicle.



**Figure 29.** Warm vehicle leaving the parking lot. The exhaust system of this vehicle appears to be hot, however because there is no reflection on the road surface on the snow, the status of this vehicle cannot be clearly determined.

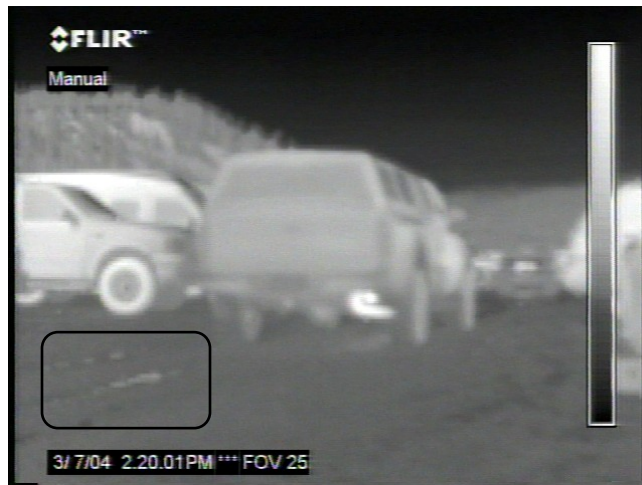


**Figure 30.** Hot truck on snow. The exhaust system of the vehicle is hot as well as the sidewalls of the tires. In the boxed area, some of the snow has melted, and water is reflecting a bright infrared object.



**Figure 31.** Cold SUV leaving the parking lot. The SUV in this figure looks very similar to the Breckinridge Ski Patrol vehicle; however the hot looking tire wall is due to heating by the sun and not by being driven. This can be determined because the other tire walls do not look hot.

## Images on Hot Road Surfaces

When the camera was set up in Las Vegas, NV on 05 May 2004 (Figures 32-38), the road surface temperature was 122°F at 10:00 AM. The scale on the camera was set in the typical fashion, however, due to the excessive heat; the images appeared to be almost completely white with very little contrast between objects in the FOV. At times the reflected heat from the underbody of the vehicle is recorded as the same brightness as the road surface, and makes it difficult to tell the difference between the reflection and the road.

Another issue that arises from extremely hot road surfaces is the reflection of the sun off of the road. In some of the figures, one can see that the lane of traffic closest to the camera has a different appearance than the other lanes of traffic. This could be due to the curvature of the road surface, and therefore the sun is reflected directly at the camera.



**Figure 32.** Flamingo Road in Las Vegas, Nevada facing towards the east. The road temperature is over 120°F.



**Figure 33.** Traffic on Flamingo Road. The vehicles traveling east on are all hot and the reflections from the underbodies of the vehicles can be seen in the lanes.



**Figure 34.** Citizens Area Transit (CAT) Bus. The engine location for the bus is in the rear of the vehicle. The bus is obviously hot, and the exhaust pipe location can be seen through the body of the bus.



**Figure 35.** Hot SUV. The reflection can be seen on the road, but the right edge of the reflection blends in with the road reflection.



**Figure 36.** Cold DRI employee vehicle. This vehicle is known to have been sitting long enough to reach the ambient temperature, however the high temperature and the driving time, approximately 20 seconds, from the parking lot to the road was enough for the vehicle to warm up noticeably.





(A)



(B)



(C)

**Figure 37A-C.** Hot vehicles with the image adjusted to see the reflection from the underbody of the vehicle without interference from the road reflection.



**Figure 38.** Hot truck. The truck in this image is hot. However the reflection from the underbody of the vehicle is masked by the emission from the road.

The image can be adjusted by the operator to adjust for the very hot conditions. This is done by adjusting the level of the picture and fine tuning the span of the picture. The images in Figure 37 have been adjusted using the span and level. The reflection, tire treads, and the tailpipe and exhaust system can be distinguished better. The adjustment of the image is subjective, and therefore can be different based on the person setting up the camera. For the images that are taken on hot road surfaces, but not adjusted to distinguish the features of the vehicle, the image can be adjusted by changing the brightness of the monitor that they are being looked at.

The ambient temperature had reached 88°F by 11:00 AM, and if the vehicle was left to sit long enough, it would also be at that temperature. The vehicles do not take as long to become hot when the ambient temperature is above



80°F. Therefore, the exhaust system of a vehicle leaving the DRI parking lot is already hot when it drives past the infrared camera. This analysis and the analysis of the CE-CERT data later shows that it is very unlikely that a modern vehicle will be cold when it drives past the camera when the temperature is above 80°F.

### Cold Start on Hot Road Surfaces

A 2001 Hyundai Accent was driven around the DRI parking lot after 1:00 PM, the road temperature was 135°F (Figures 39-44). When the camera was set up, the road appeared to be very white in the image. The camera was adjusted in order to get a better look at the reflection from the underbody of the vehicle, the exhaust system, and the tire treads. As the vehicle was driven, the exhaust system and the tire treads could be seen to get brighter in the image as the vehicle warmed up. However when the road temperature is so high, it can still be hard to see the reflection from the underbody of the vehicle even with adjusting the brightness of the image. The most apparent part of the vehicle to watch is the exhaust in order to determine if the vehicle is hot or cold when the road temperatures are at 135°F.



**Figure 39.** 2001 Hyundai Accent at cold start. Approximately 10 seconds from start.



**Figure 40.** Vehicle after driving around the parking lot one time. The tires and the exhaust system have warmed up and the reflection from under the vehicle can be seen on the road surface. Approximately 49 seconds after start.



**Figure 41.** The vehicle is noticeably warmer than the previous figure. The reflection, the exhaust system, and the tire treads are brighter. This image was taken 39 seconds after Figure 40.



**Figure 42.** The exhaust system of the vehicle is still increasing in brightness.



**Figure 43.** The tailpipe of the vehicle is very noticeable; however the reflection does not appear to be getting any brighter.



**Figure 44.** The tailpipe is the brightest object in the image, and the vehicle is fully warmed up. The reflection seems to have reached its brightest more than a minute previous to this image, but the tailpipe continued to get hotter.

When replaying the video, it was noticed that if the vehicle had stopped for several seconds and then started to go around the parking lot, there appeared to be a dark area where the vehicle had stopped. The area was approximately the same size as the reflection from the vehicle, and was due to the vehicle blocking the sun from warming up the pavement.

On days when the ambient temperature is hot and the roads are hot, vehicles warm up fast when compared to cold days. The reflection is harder to see because the road emits more infrared radiation, which then blends in with the vehicle's reflected infrared radiation. However, because the vehicle light-off times are faster, the ability to see the reflection is less important.

### Results from the Regis High School Experiment

The videotapes were played and watched to decide if the vehicle was hot or cold. A vehicle grade of GOOD, FAIR, or POOR was assigned based on the cut off for CO from the Smart Sign. If a vehicle had emissions that were FAIR, and the vehicle looked significantly hot compared to vehicles that drove by before and after the said vehicle, then the vehicle was put into the hot category. If a vehicle appeared to be on the cool side, then the vehicle was designated as cold. A vehicle was only put into the POOR/hot category if it was significantly hot compared to other vehicles that pass the FEAT unit around the same time. The idea was to evaluate the extent to which high emitting vehicles that are hot could

be positively identified, and, most importantly, exclude any vehicle that is putting out high emissions because it is not fully warmed up.

The majority of the vehicles in this experiment were driven by sophomore and junior boys that attended the school. The vehicles were observed at the end of the school day, and the rate of acceleration that the vehicles were driven may have had an effect on the emissions that were observed from the tailpipe. The speed and acceleration bars that are typically used to correct for this were not used for this experiment, but it is believed that the emissions are not very different from the true emissions.

From the study at Regis High School parking lot, 332 vehicles were tested, of which 74% were cold, and 24%, were hot by visual interpretation of the images. Vehicles were driven past the FEAT unit within about 30 seconds of being started. While this is close to the time needed for light-off, the temperature was near 40°F. As the temperature decreases, the light-off time increases. Some of the vehicles sat in the parking lot with the engine on prior to getting emissions measurements; however, a majority of the vehicles were started and driven out of the parking lot. Of the 332 vehicles, 62 received a poor rating, or approximately 20% of the vehicles. About half of the vehicles that were tested, both hot and cold, received a good rating, and the other third of the vehicles rated as fair. There was only one vehicle out of 332 that received both a POOR rating and was hot based on the IR image. Figure 45 shows a summary of these results.

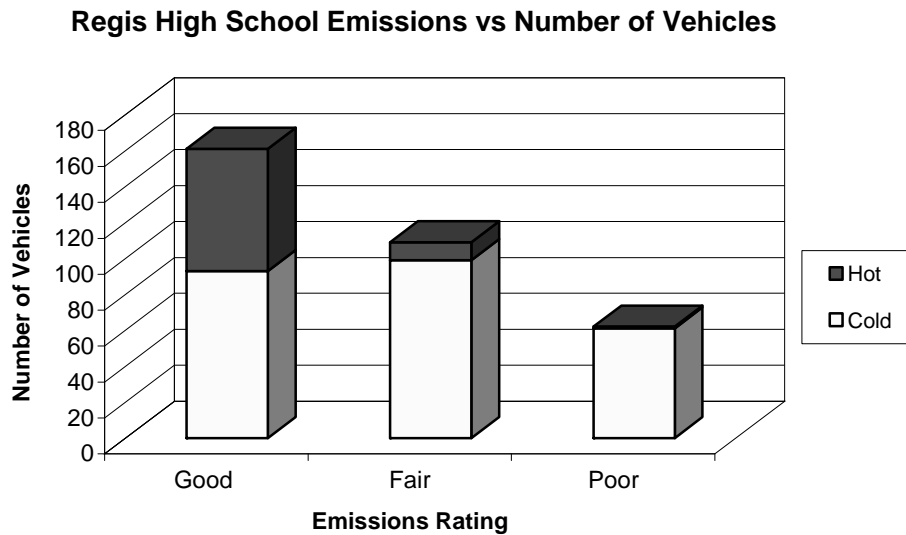


**Figure 45.** Results from Regis High School parking lot. The results include the data from all vehicles that were measured on two consecutive days.

For properly operating vehicles, cold vehicles are likely high emitters while hot vehicles are unlikely high emitters. The infrared camera can be used to distinguish between the two scenarios in order to ensure that cold vehicles are not identified incorrectly as repairable high emitters. Table 1 shows these results. When the vehicle is cold started, there will often be a higher emission of CO and unburned HC when the vehicle is measured. This was verified by the Regis High School results. Also, when vehicles are hot, there is a small probability that the vehicle is high emitting, and therefore it was expected that very few of the vehicles from the experiment at the high school would rate poor.<sup>16</sup> This hypothesis was verified.

	<1.0%CO	1.0 ≥ %CO < 3.5	%CO ≥3.5
Cold	93	99	61
Hot	68	10	1
Expected Hot <sup>16</sup>	73 (93%)	4 (5%)	2 (2%)

**Table 1.** This table shows the number of vehicles that received a GOOD, FAIR, or POOR rating, as well as if the vehicle was a cold or hot vehicle. From the data of both days of measuring vehicles at the high school, there was only one vehicle received both a POOR rating and was a hot vehicle.

Of the 332 observed vehicles at Regis High School, there were 79 hot vehicles and 253 vehicles were cold as determined from the infrared images. This result was anticipated because it was known that the vehicles had been sitting for approximately six hours, thus most of the vehicles were expected to be cold when they passed the FEAT unit at 3 PM. The 253 cold vehicles produced many more FAIR and POOR readings than a normal Denver hot vehicle fleet, as was expected. Based on contemporary Smart Sign data at Speer Boulevard and I-25 where all of the vehicles are warm, the expected ratio of GOOD, FAIR, and POOR readings for a fully warmed up vehicle are known.<sup>16</sup> The expectation is that out of 79 hot vehicles, 73 would receive a GOOD, 4 would receive a FAIR, and 2 would receive a POOR rating from the Smart Sign.<sup>16</sup> The vehicles that received the hot and POOR rating may have warmed up a bit in the parking lot, but may not have reached light-off when their emissions were measured. The observed distribution of 68:10:1 indicates that the difference between hot vehicles with high emissions and the cold vehicles with high emissions could be



differentiated. The hypothesis that the camera and infrared imaging technique can be used to distinguish between hot and cold starts is confirmed.

The images in Figures 46-49 are all cold start vehicles; however, the vehicles in Figures 46 and 47 is already a low emitting vehicles, while in Figures 48 and 49 the vehicles are still high emitting. This shows that even though vehicles are cold, they are not necessarily high emitting. Figure 50 shows a truck that is both hot and has low emissions.



**Figure 46.** Cold start with 0.95 %CO.



**Figure 47.** Cold start with low emissions. The %CO is 0.92.



**Figure 48.** Cold start with 3.85 %CO.



**Figure 49.** Cold start with high emissions. The %CO is 3.07. This vehicle would be classified as a repairable high emitter without the IR camera.



**Figure 50.** Hot truck with 0.34 %CO.

## Comparison of Cold Starts

Blue (MY 1986) took 224 seconds to fully warm up (road temperature of 24.5°F, Figures 16-18), while it appeared to take the Hyundai only 75 seconds to fully warm up (road temperature of 135°F, Figures 39-41). The warm up time for Blue is known because there are FEAT data to confirm that the emissions are stabilized. The Hyundai does not have any emissions data for this particular experiment; however this vehicle is known to be a low emitting vehicle and the emissions should be stabilized before 75 seconds. A direct comparison of these two vehicles would need emissions data along with the infrared imaging. Vehicles that start at lower ambient temperatures, such as temperatures below 40°F, take longer to reach light-off.

It requires more careful camera set-up to observe the differences between the road surface and the reflection from the road surface when the road is 135°F. When the road surface less than 100°F, the differences are much easier to see between the road and the reflected heat from the underbody of the vehicle.

## Quantitative Analysis of the Infrared Images

An added benefit of using grayscale infrared images is that there is only one variable, pixel intensity. When the road temperatures were cold, there was more of an obvious contrast between the road surface and the reflection from the underbody of the vehicle. As the vehicle became hotter, the reflection become

brighter. Vehicles at cold start had either no reflection or very little reflection, depending on the road surface temperature, and the pixel intensity was close to that of the road surface. As the vehicle temperature increased, the reflected infrared became brighter and the amount of black per pixel decreased and there was a greater difference from the pixel intensity of the road surface.

From the histogram, the mean of the selected pixels for a hot vehicle approached 255 while the cold road or cold vehicle approached 100; however the lowest observed road intensity or cold vehicle intensity was 68. The reflected heat from the underbody of the vehicle adds average intensity to that normally received from the road (Equation 11).

The contrast ratios that were calculated using equations 10 and 11 on pages 35-36, range from 1.85 (cold start in Las Vegas) to 3.85 (cold road study next to Cherrington Hall). The colder the road surface, the higher the contrast ratio is between the road surface and the reflection from the underbody of a hot vehicle. When the road is hot, as it was in Las Vegas, then there is less contrast between the road and the road plus the reflection under the vehicle; therefore the contrast ratio decreases. The graph in Figure 51 illustrates this trend. The contrast ratio decreases in a cold start case where there is almost no reflection from the underbody of the vehicle.

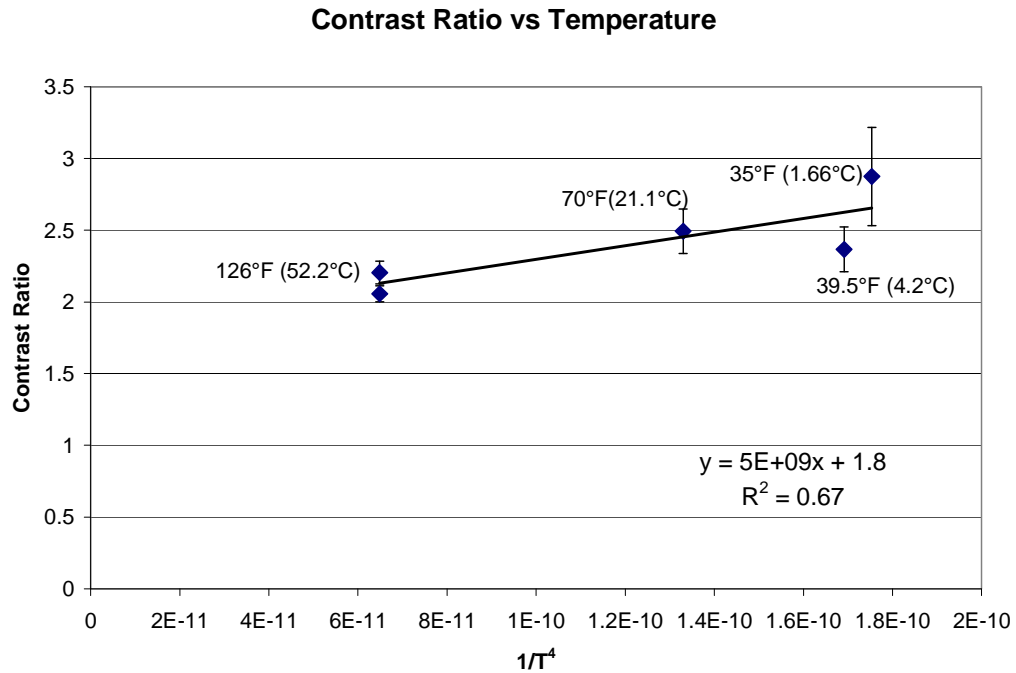


**Figure 51.** Graph of hot vehicle contrast ratio versus  $1/T^4$ . As the road surface temperature increases, the contrast ratio decreases. The uncertainty bars are the standard deviation of the data.

There are two points for a road temperature of 126°F. This is because some of the images were adjusted to be darker and show on the video screen more contrast between the reflection and the road surface. The average contrast ratio for the images that were not adjusted to be darker is 2.05 while the adjusted images had a contrast ratio of 2.20. Both ratios are very close which suggests that all of the necessary information was not lost when changing the level of the image. This also demonstrates that little or no information was lost from transferring the images from analogue to digital and then using the Photoshop

software to obtain the contrast ratios. Figure 51 illustrates that the expected loss of contrast at high temperature is observed. The trend does not follow Equation 11. This is not surprising in view of the fact that the level and span of the camera are reset for each study, and Equation 11 is oversimplified since the emissivity of the road surface and the angle of reflection are not taken into account. Also, emissivity and reflectivity of the road surface may differ between sites in Denver and Las Vegas.

### Reanalysis of Data from Younglove, *et al.*

Out of the 348 vehicles in the data set, only 246 had FTP data which were helpful to use. Vehicles that had invalid data or vehicles not equipped with a catalyst were not considered. An example of a (CO/CO<sub>2</sub>) versus time graph is given in Figure 52. From these data the 90% recovery of the emissions is found. The vehicle that was tested in this FTP was a 1995 Jeep Cherokee, which was very cleanly emitting at the time of this FTP. Once the vehicle's oxygen sensor had sufficiently warmed up, the vehicle's emissions became steady. A majority of the vehicle data that were analyzed displayed similar second by second data.

Not all of the vehicles in the data set showed a peak and smooth decline in the amount of CO that is emitted from the vehicle. Some vehicles emit a variable amount of CO based on the mode of the vehicle, i.e. full power mode. In Figure 53 from a 1985 Chevy Spirit, the emissions start out at what the Smart Sign would

designate as POOR, but reduce to the GOOD grade with time. The vehicle exhibits variability in the amount of CO that it emits during different driving cycles. While this vehicle is an outlier in the data set, there were other vehicles that had similar second by second data.

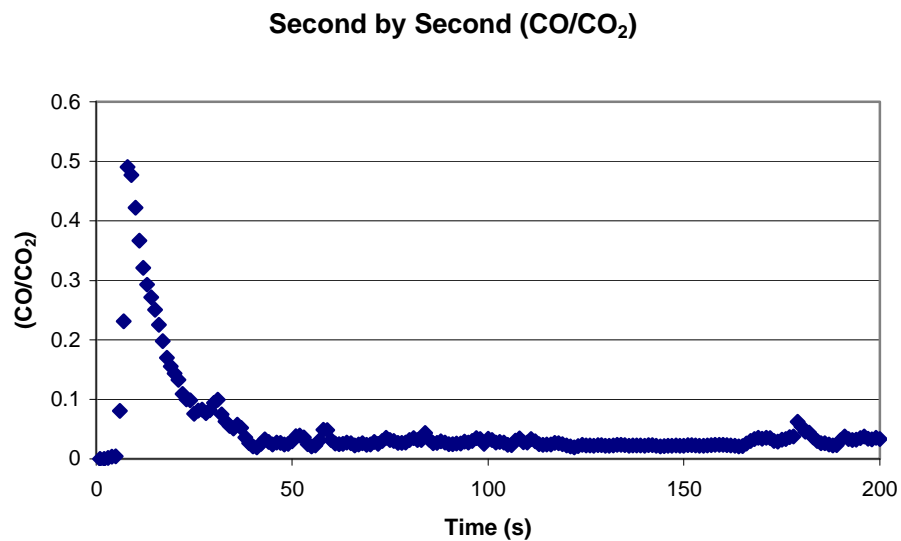


**Figure 52.** Typical graph of 200 seconds of the second by second (CO/CO<sub>2</sub>) data from FTP Bag 1 for a 1995 Jeep. The 90% recovery emissions are 0.067 (CO/CO<sub>2</sub>), and the time to reach 90% recovery is 28 seconds.<sup>10</sup>



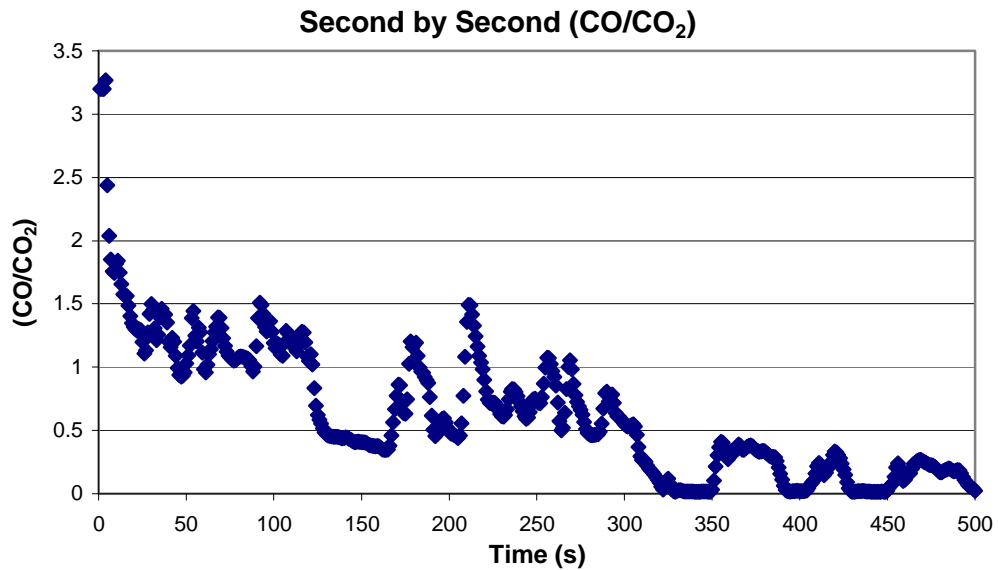


**Figure 53.** Second by second data for a 1985 Chevy Spirit. This vehicle has high emissions when started, but decreases to an acceptable amount as the vehicle is driven. The amount of CO that is emitted is variable based on the driving cycle. The 90% recovery emissions are 0.42 (CO/CO<sub>2</sub>) and the time it took to reach 90% recovery was 144 seconds.<sup>10</sup>

After all of the 90% recovery times were derived, the average time was found for all vehicles to be 27.7 seconds. The averages for five year bins, with the exception of 1977-1984 due to the small number of vehicles, was also determined (Figure 54). The average time to 90% recovery for the oldest vehicle bin is 47.6 seconds. For the newest vehicles that were tested the average time to 90% recovery was 24.3 seconds. The older the vehicle, on average, the longer it takes for the catalyst to light-off. From this graph, there is a trend that newer vehicles achieve shorter light-off times than older vehicles, and vehicles produced

after 1999 would be expected to display even shorter light-off times based on newer technology.

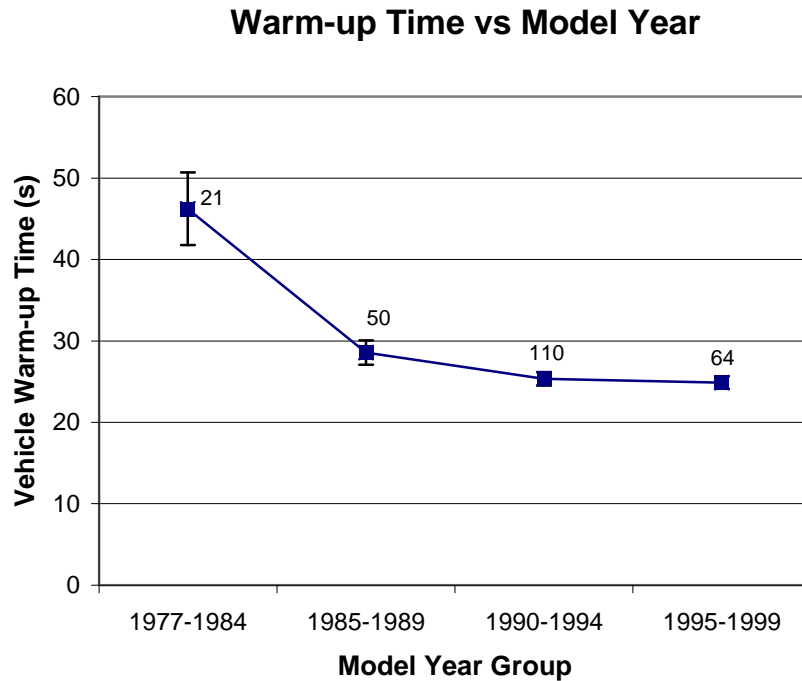


**Figure 54.** Graph showing warm up times derived from of the FTP data put into five MY bins, with the exception of 1977-1984, comparing 90% recovery warm up times vs. MY. The uncertainty bars are the standard errors of the mean. The data labels are the number of vehicles in each MY bin.

These trends are in agreement with Younglove, *et al.* 1999, who state that “...light-off times were found to be decreasing with newer model years.”<sup>13</sup> However, the analysis using the 90% recovery of emissions gives average light-off times of 24-26 seconds for vehicles from 1990-1998 MY range. The light-off times derived by this method are shorter than those derived from the more complex algorithm developed by Younglove, et al.

	GOOD	FAIR	POOR
90% Recovery Emissions	28	181	37
Baseline Emissions	230	13	3
Expected Hot <sup>16</sup>	229 (93%)	12 (5%)	5 (2%)

**Table 2.** This table gives the number of vehicles that received a GOOD, FAIR, and POOR rating, based on the %CO tailpipe emissions, at the time it took the vehicle to reach 90% recovery of the maximum emissions as well as the number of vehicles that received these ratings at the baseline emissions.

For the 246 vehicles analyzed by the 90% recovery method, very few of the vehicles (28) had reached <1.0 %CO, and there were a significant number of vehicles (181) in the FAIR category at 90% recovery. CE-CERT recruited about 40% of their test fleet to be high emitters, therefore a significant number of vehicles were dirty. By the time that the vehicles reached their baseline emissions all 246 vehicles fell within the expected distribution of GOOD, FAIR, and POOR ratings. This reanalysis of the data leads to shorter warm up times than the CE-CERT light-off times, it is speculated that this arises because the oxygen sensor is the time limiting factor for major control the vehicle emissions.<sup>12</sup> This is due to the placement of the oxygen sensor in the exhaust manifold. The hot exhaust gases reach the oxygen sensor much faster than they reach the catalyst.

The short warm up times derived from this analysis are important because 25 seconds is rarely a long enough time to reach a public road way from cold start. It should be noted that the FTP studies are done at a controlled temperature

of 75°F. At a warmer temperature, the warm up time will be even shorter and so the probability of finding a cold start vehicle by using remote sensing when the temperature is above 80° or 90°F is very small. This is advantageous because hot roads are hard to deal with in the infrared. At colder temperatures the warm up times will be longer, but the use of the infrared camera to identify these cold start vehicles is increasingly easy as the temperature decreases.

## Conclusions

While it was known that road surfaces can reflect infrared radiation from the underbody of the vehicle onto the road surface, the ability to usefully evaluate this information with a commercially available camera under different road conditions was not known. There was enough contrast in approximately 40 hours of images analyzed to determine if vehicles were hot or cold by visual inspection. The contrast ratios give conformation of this, and are useful to help determine the status of the vehicle when compared to other vehicles that have driven by recently. When the contrast ratio is high, then the vehicle is hot, and when the ratio is low, especially when compared to vehicles that pass by the camera fairly soon after or shortly before a specific vehicle, then the vehicle is cold.

On hot days, when the road temperature is above 110°F, there is very little obvious contrast between the road and reflection from the underbody of the vehicle. Careful camera adjustment can improve the visual image quality. However, a quantitative, software derived contrast ratio can also help to determine the status of the vehicle on hot days. However, the probability of a cold start vehicle driving past the on-road remote sensor is very low on hot days. On cold days, which are more likely to have cold vehicles drive past a remote

sensor, the contrast ratio between the road surface and the reflection from the underbody of the vehicle is greater and more readily visibly observable.

During this project, it was determined that snow covered roads do not work well for this application of the infrared camera. The snow absorbs the reflected heat from the underbody of the vehicle as well as cools the tire treads. Therefore it is a poor surface to determine the hot/cold status of a vehicle. However, if it is snowing (or raining) the remote sensor will not report valid emissions from vehicles because precipitation adds unacceptable noise to the analyzer beam intensities.

The reanalysis of the CE-CERT data agrees with the original analysis in that there is a trend for the light-off time to increase as the vehicle ages. However, the new derived length of time for warm up differs from CE-CERT. While CE-CERT derived catalyst light-off times of 40-80 seconds, Figure 54 shows emissions warm up times averaging from 25-50 seconds. As the technology gets better, the expected light-off and warm up times should decrease further. Thus, newer vehicles are expected to achieve even faster light-off and warm up times.

## **Future Research and Development**

Eventually, the use of the infrared camera will be incorporated into the remote sensing devices, used in High Emitter Identification (HEI) programs. In these programs, video images are used to obtain the license plate of the vehicle with an eventual goal of giving citations to the owners of hot high emitting vehicles. The video and infrared images will be saved digitally. An effective program would involve software that does not save every infrared image, but saves the infrared images that precede and follow a high emitting vehicle. With this capability, an inspector would be able to compare the infrared image of the high emitter with other vehicles that are not high emitting but do share the same road surface and light conditions.

## References

1. Heywood, J. B. *Internal Combustion Engine Fundamentals*: McGraw-Hill: New York, NY, 1988.
2. Mondt, J. R. *Cleaner Cars: the History and Technology of Emission Control since the 1960s* Society of Automotive Engineers: Warrendale, PA, 2000.
3. Larson, R.E. Vehicle Emission Characteristics under Cold Ambient Conditions, Society of Automotive Engineers Publication # 890021, **1989**, 151-159.
4. National Research Council. *Modeling Mobile Source Emissions*; National Academy Press: Washington, D. C. 2000.
5. Bridges, J. L.; Hanna, W. C., *Quantifying the Effects of Oxygenated Gasoline on Cold Start Automobile Emissions*, Proceedings of the Air and Waste Management Association, Atlanta, GA, October 11-15, 1993.
6. Stedman, D. H.; Bishop, G. A. Apparatus for Remote Analysis of Vehicle Emissions Using Reflective Thermography. U. S. Patent 5,489,777, Feb. 6, 1996.
7. FLIR ThermoVision A20V Operator's Manual, FLIR Systems, Inc.
8. Joumard, R.; Vidon, R.; Paturel, L; de Soete, G. Changes in Pollutant Emissions from Passenger Cars under Cold Start Conditions, Society of Automotive Engineers Publication #961133, **1996**, 23-34.
9. Laurikko, J. K. Automotive Exhaust Emissions at Low Ambient Temperature, Society of Automotive Engineers Publication # 890003, **1989**, 35-46 .
10. Barth, M. J.; An, F.; Younglove, T.; Scora, G.; Levine, C.; Ross, M.; Wenzel, T. *Development of a Comprehensive Modal Emissions Model*. Final Report NCHRP Project 25-11, April, 2000.
11. Dynamometer Drive Schedule Quick View  
<http://www.epa.gov/otaq/emisslab/methods/quickdds.htm> (June 25, 2004).



12. Yoo, J.; Bonadies, J. V.; Detwiler, E; Ober, M; Reed, D. A Study of a Fast Light-Off Planar Oxygen Sensor Application for Exhaust Emissions Reduction, Society of Automotive Engineers Publication # 2000-01-0888, **2000**, 1-8.
13. Younglove, T.; Levine, C.; Barth, M. J.;Scora, G.; Norbeck, J. M. In *Analysis of Catalyst Efficiency Differences Observed in an In-Use Light Duty Vehicle Test Fleet*, Proceedings of the CRC, San Diego, CA, April 19-21, 1999.
14. Bishop, G. A.; Stedman, D. H. Measuring the Emissions of Passing Cars, *Acc. Chem. Res.* **1996**, 29, 489-495.
15. *On-Road Remote Sensing of Automobile Emissions in the Chicago Area: Year 1*, P.J. Popp, G.A. Bishop and D.H. Stedman, Final Report prepared for CRC, August, 1998.
16. Smart Sign Homepage [www.sign.du.edu](http://www.sign.du.edu) (July 10, 2004).
17. FEAT Homepage [www.feat.biochem.du.edu](http://www.feat.biochem.du.edu) (June 22, 2004).
18. Burns, D. A., Ciurczak, E. W., Eds. *Handbook of Near-Infrared Analysis*; Marcel Dekker: New York, NY, 2001.
19. Earth Observatory: On the Shoulders of Giants  
[http://earthobservatory.nasa.gov/Library/Giants/Langley/langley\\_2.html](http://earthobservatory.nasa.gov/Library/Giants/Langley/langley_2.html)  
(July 6, 2004).
20. Levine, I. N. *Quantum Chemistry*: Prentice Hall: Upper Saddle River, NJ, 2000.
21. Atkins, P. de Paula, J. *Quantum Theory: Introduction and Principles. Physical Chemistry*, 7<sup>th</sup> Edition; W. H. Freeman, New York, 2002.